Bulletin of the Geological Society of Finland, Vol. 90, 2018, pp 5–32, https://doi.org/10.17741/bgsf/90.1.001

Characterization and origin of dunitic rocks in the Ni-Cu-(PGE) sulfide ore-bearing Kevitsa intrusion, northern Finland: whole-rock and mineral chemical constraints

Kirsi Luolavirta[1*], Eero Hanski[1], Wolfgang Maier[2] and Frank Santaguida[3]

[1] *Oulu Mining School, University of Oulu, P.O.BOX 3000, FI-90014, Finland*
[2] *School of Earth and Ocean Sciences, Cardiff University, Cardiff CF10 3AT, UK*
[3] *First Cobalt Corp. Suite 201, 140 Yonge Street, Toronto, Canada*

VERTAISARVIOITU
KOLLEGIALT GRANSKAD
PEER-REVIEWED
www.tsv.fi/tunnus

Abstract

The ca. 2.06 Ga Kevitsa intrusion is one of the ore-bearing mafic-ultramafic igneous bodies in the Central Lapland greenstone belt. A large disseminated Ni-Cu-(PGE) sulfide ore deposit is hosted by olivine-pyroxene cumulates in the lower ultramafic part of the intrusion, indicating involvement of a multiply saturated magma in the ore formation. There are also various dunitic rocks, which occur as numerous inclusions within the Kevitsa intrusion, most commonly in the economic resource area. On textural basis, two distinct types of inclusions are recognized: i) cumulate-textured (Kevitsa Dunite) and ii) recrystallized ultramafic inclusions. In addition, there also exists a separate dunitic body (Central Dunite) with a suface area of 0.6 x 1.0 km, cropping out in the central part of the intrusion.

The Central Dunite and Kevitsa Dunite are similar olivine-chromite cumulates and with comparable whole-rock and mineral compositions, suggesting that they are cogenetic. A magmatic, rather than replacement origin for the dunitic cumulates is evidenced by their systematic mineral compositional trends consistent with magmatic fractionation. Whole-rock major and trace element and mineral compositional data of the dunitic cumulates and Kevitsa olivine pyroxenites fall on the same linear trends and record similar REE characteristics indicating a genetic link between these two. The parental magmas for the dunitic cumulates were probably picritic and related to the picritic and basaltic volcanic rocks in the area. The high Fo content of olivine (up to ~89 mol.%) is consistent with a high-Mg parental melt.

The recrystallized ultramafic inclusions are fine-grained and show a granoblastic/interlobate textures indicative for thermal textural readjustment. Two subgroups are identified: Group 1 shows a chemical affinity towards the dunitic cumulates and are interpreted as their recrystallized clasts. The Group 2 inclusions are compositionally comparable to the ~2.06 Ga komatiitic volcanic rocks in the area and are considered as dehydrated metavolcanic xenoliths. A decrease in the flow rate of the Kevitsa magmas due to entrapment of a high number of inclusions is proposed as a mechanism to promote settling of sulfides, contributing to the formation of the Ni-Cu-(PGE) ore.

Keywords: dunite, ultramafic rock, thermal recrystallization, geochemistry, mineral composition, inclusion, Ni-Cu-PGE sulfide ore, Kevitsa intrusion, Paleoproterozoic, Finland

*Corresponding author (e-mail: kirsi.luolavirta@student.oulu.fi)

Editorial handling: Jussi S. Heinonen (jussi.s.heinonen@helsinki.fi)

1. Introduction

Within the Earth's crust, dunite may form by primary magmatic (cumulate) processes within mafic-ultramafic magma chambers and magma conduits. Such cumulate dunites have been described, e.g., from the Monchegorsk (Sarkov & Chistyakov, 2012) and Burakovsky (Chistyakov & Sarkov, 2008) layered complexes in Russia, Muskox layered intrusion in Canada (e.g., Day et al., 2008), Stillwater complex in USA (Raedeke & McCallum, 1984), Koitelainen layered intrusion in Finland (Mutanen, 1997) and Jinchuan ultramafic intrusion in China (Chai & Naldrett 1992). The formation of the dunites is generally related to fractionation of olivine and its accumulation at the basal parts of the intrusion or at the base of individual cyclic units, which are often interpreted to have resulted from new primitive magma pulses into a magma chamber. At Jinchuan, dunites are also found in the interior of a magma conduit thought to have formed as a consequence of flow differentiation of a magnesian magma (Chai & Naldrett, 1992). On the Earth´s surface, dunites may also form at the base of high-magnesian (komatiitic) lava flows (e.g., Barnes et al., 1988). In addition to cumulate processes within intrusive bodies, magmatic infiltration and replacement (metasomatism) at the expense of other ultramafic lithologies may account for the generation of some dunitic bodies. Such replacement dunites have been described from well-studied intrusive suites in the Stillwater complex, (McCallum, 1996) and Duke Island (Irvine, 1974), for example, where they are recognized by their common pegmatoidal textures and irregular and/or transgressive relationships to the primary layering. In the Bushveld complex (South-Africa), dunites are found as pipe-like bodies aligned roughly perpendicular to the layered rocks. Scoon & Mitchell (2004, 2009) considered them to have originated via flow differentiation of relatively late mafic/ultramafic magmas injected into the adjacent semi-consolidated cumulates whereas Schiffries (1982) and Stumpfl & Rucklidge (1982) proposed a replacive origin for dunite pipes rich in PGEs.

The ore-bearing Kevitsa intrusion is one of the Paleoproterozoic mafic-ultramafic intrusive bodies in the Central Lapland greenstone belt, emplaced into a supracrustal sequence containing pelitic metasediments and mafic-ultramafic metavolcanic rocks (Mutanen, 1997; Santaguida et al., 2015). A low-grade but very large Ni-Cu-PGE ore body occurs within the central part of the ultramafic cumulate zone, rather than at its bottom, as is the case for many other magmatic Ni-Cu sulfide ore deposits (cf. Barnes & Lightfoot, 2005). Given the mafic-ultramafic nature of the intrusion, the bulk sulfide is relatively rich in Cu, having Ni/Cu <1. On the other hand, there exists a subordinate ore type that is extremely rich in Ni, with the Ni tenor approaching 40 wt.% (Yang et al., 2013).

A peculiar feature of the Kevitsa intrusion is the presence of numerous ultramafic, olivine-dominated inclusions. These inclusions occur as distinct raft-like dunitic cumulate body(s) up to several tens of meters in thickness (Kevitsa Dunite) and as small, fine-grained, recrystallized ultramafic inclusions within the Kevitsa olivine-pyroxene cumulates. Interestingly, inclusions are most abundant within the ore-bearing domain of the intrusion, implying a possible linkage to the ore formation. In addition, a large, km-sized dunitic body (Central Dunite) crops out in the gabbroic zone and is also intersected by drilling at the bottom of the intrusion.

Neither the inclusions nor the Central Dunite have been studied in detail and their origin remains controversial. Mutanen (1997) interpreted the ultramafic inclusions (including the Central Dunite) as komatiitic country rock xenoliths and more recently, Yang et al. (2013) related them to an early-stage komatiitic magmatism with a close temporal link to the emplacement of the Kevitsa intrusion. However, textural features and compositional variations of the inclusions as well as their occurrence within the central part of the intrusion require alternative explanations for their origin. In particular, the potential genetic relationship between the dunitic cumulates (the Central Dunite and Kevitsa Dunite) and

the Kevitsa ultramafic succession as part of the magmatic emplacement history of the Kevitsa intrusion requires evaluation. In this paper, we present drill core observations and petrological data from various dunitic rocks in the Kevitsa intrusion. We utilize mineralogy and the whole-rock and mineral chemical data to access the origin of the dunitic cumulates and the recrystallized ultramafic inclusions and discuss the magmatic history of the Kevitsa igneous suite. The potential relationship of the inclusions to the Ni-Cu sulfide ore genesis is also addressed.

2. Geological background

The sulfide ore-bearing Kevitsa intrusion is located within the Central Lapland greenstone belt (CLGB), northern Finland, 34 km north of Sodankylä (Fig. 1). The CLGB is mainly composed of komatiitic to rhyolitic metavolcanic rocks, mafic-ultramafic intrusions and sedimentary rocks and records a Paleoproterozoic geological evolution from ca. 2.5 Ga to 1.8 Ga. The geologic history of CLGB is summarized by Hanski & Huhma (2005).

The Kevitsa magma intruded into pelitic metasediments and metavolcanic rocks of the Savukoski Group (Lehtonen et al., 1998) at ca. 2058 Ma (Mutanen & Huhma, 2001). The volcano-sedimentary rocks in the area comprise phyllites, black shales, mafic tuffs and mafic to ultramafic lava flows. The komatiites of the Savukoski Group, which occur together with picritic volcanic rocks, have yielded a Sm-Nd age of 2056 ± 25 Ma (Hanski et al., 2001) being similar to the age of the Kevitsa intrusion.

The Kevitsa intrusion is a relatively small intrusive body with a surface area of approximately 16 km^2. It is composed of a ~1.5-km-thick ultramafic lower part overlain by ~500 meters of gabbroic rocks (Mutanen, 1997; Fig. 2). The ultramafic part is dominated by relatively uniform olivine (10–30%) – clinopyroxene (65–85%) cumulates with variable amounts of orthopyroxene oikocrysts (2–15%). Orthocumulate-textured plagioclase-bearing olivine websterites and fine-grained microgabbros occur as discontinuous south-north–trending zones within the olivine pyroxenites in the central part of the intrusion. Olivine pyroxenites grade into pyroxenites (websterite/clinopyroxenite) towards the top of the ultramafic zone. The marginal series rocks at the base of the Kevitsa intrusion comprise pyroxenites (±olivine) and gabbros.

A large dunite body, referred to as the Central Dunite, crops out in the middle of the Kevitsa intrusion (Figs. 2, 3a). Dunite has also been intersected in some drill holes at the base of the deepest parts of the Kevitsa intrusion (Fig. 3b). Reflection seismic measurements (Koivisto et al., 2015) and the mineralogy of these "footwall" dunites (this study) indicate that they are part of the Central Dunite. Dunitic cumulates (termed the Kevitsa Dunite) also occur within the olivine pyroxenites in the area of the ore deposit (Fig. 3b). In addition, small, cm-scale fragments of recrystallized ultramafic rocks are found scattered around the Kevitsa intrusion, being most common within the ore deposit.

The Kevitsa Ni-Cu-PGE deposit is made up of disseminated sulfides that occur in the center of the ultramafic portion of the intrusion (Fig. 3). The mineralization is divided into two economic end-member ore types (Mutanen, 1997): the regular Cu-Ni ore with Ni/Cu <1 and the Ni-PGE ore with Ni/Cu commonly >5. The intrusion also contains intermediate ore types (transitional ore). In addition, there are metal-poor "false ores" and contact mineralization, which are both uneconomic. Besides metal tenors, the ore types show differences in their REE contents and isotopic compositions (Hanski et al., 1997; Grinenko et al., 2003). The Ni-PGE ore is distinct from the other ore types by its more forsteritic and nickel-rich olivine (up to 14 000 ppm Ni, Mutanen, 1997; Yang et al., 2013). The regular ore type comprises the most important economic resources, whereas the volume of Ni-PGE ore is far less significant.

Isotopic signatures and trace element characteristics of the Kevitsa intrusive rocks indicate that

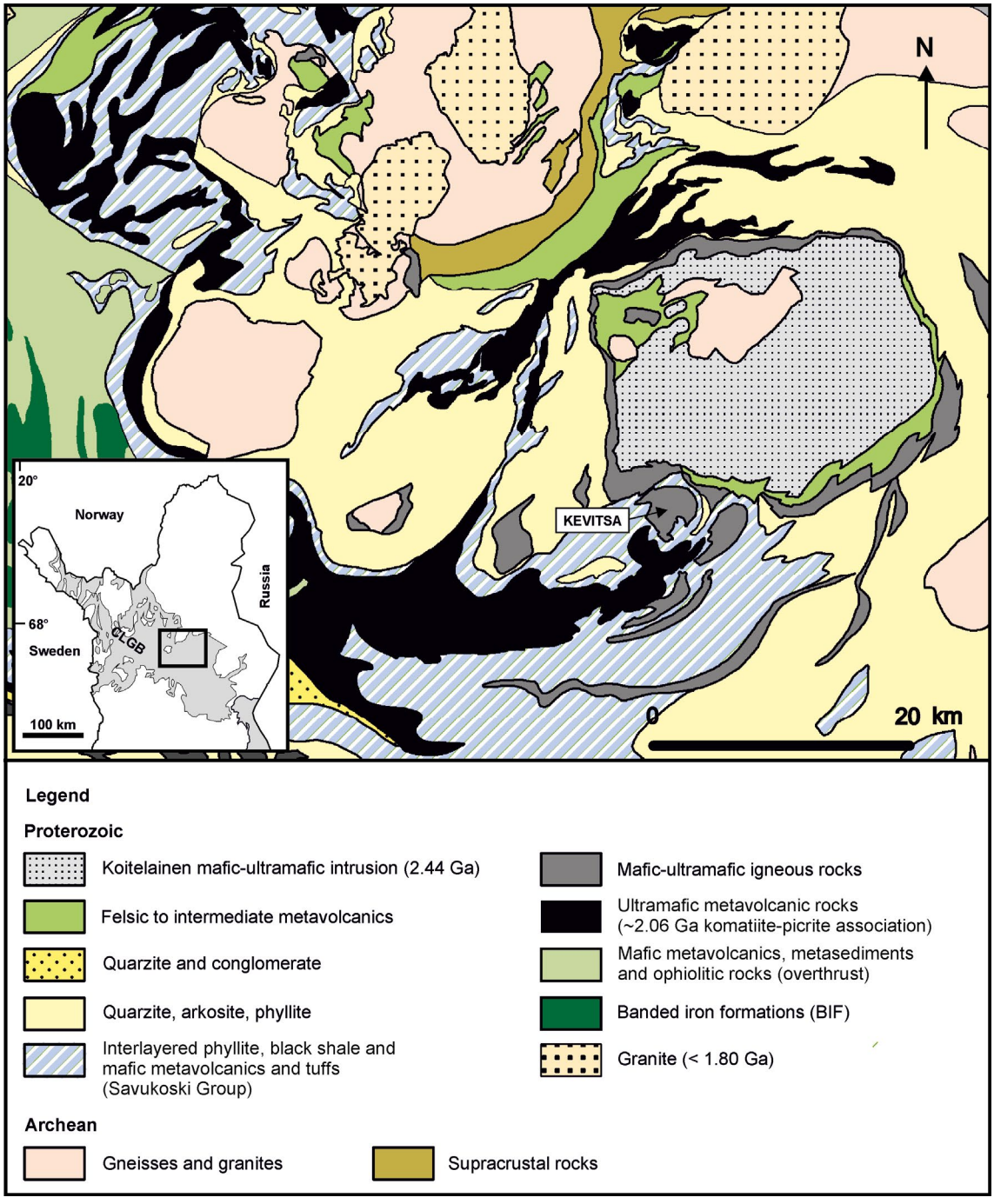

Figure 1. Geological map of part of the Central Lapland greenstone belt, showing the location of the Kevitsa intrusion and associated mafic-ultramafic intrusive bodies and ultramafic volcanic rocks. Modified after DigiKP, the digital map database of the Geological Survey of Finland, available at: http://gtkdata.gtk.fi/Kalliopera/index.html).

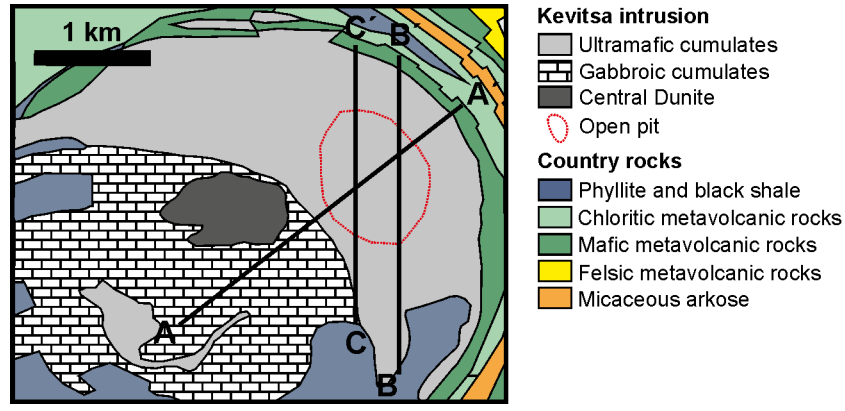

Figure 2. Geological map of the Kevitsa intrusion. The boundaries of the open pit shows roughly the location of the ore deposit. Also shown are the locations of the cross sections A-A', B-B' and C-C' of Figs. 3a-c.

assimilation of crustal rocks and input of external sulfur played important roles in the generation of the ore-bearing intrusion. This is supported by the low initial ε_{Nd} values from -6.4 to -3.4 obtained for barren and sulfide-bearing samples (Hanski et al., 1997; Huhma et al., unpublished data) and heavy $\delta^{34}S$ values from +4 to +8.2 measured for different ore types (Grinenko et al., 2003).

3. Sampling and analytical methods

The large lithogeochemical data base of the Kevitsa mine includes data produced in a commercial laboratory (ALS Ltd/Labtium Oy) and Chemical laboratory of Geological Survey of Finland (GTK, former Labtium Oy). Whole-rock major and trace element concentrations were determined by XRF using fused beads (ALS Ltd) or pressed powder pellets (Labtium Oy, GTK) and by ICP-MS/ICP-AES using a 4 acid digestion method. Loss on ignition values are available for the majority of the XRF samples. The quality of the data is monitored by repeated analyzes of certified (e.g. STSD-4, SY-4, QCGBMS304-6) and internal reference materials. The data of the standards must fall within the range of acceptance, which is generally ±5% but can be up to ±20% for certain trace-elements. For further details about the analytical methods, precisions and detection limits see Rasilainen et al. (2007) and visit the ALS Ltd (analytical codes ME-MS61, ME-XRF06) and Labtium Oy (analytical codes 175X, 306PM) Web sites. Some analytical bias may arise due to the number of data sources and multiple separate batches of analysis. In this study, we primarily utilize the XRF and REE data provided by the mine.

The locations of the drill cores from which the majority of thin section samples were collected and from which whole-rock chemical data are utilized are shown in Fig. 3. Thin section samples of Central Dunite (13 pcs.) are collected from drill cores KV201, KV305 and KV28 and R340, Kevitsa Dunite from KV156, KV148 and KV34 (9 pcs.), Group 2 inclusions from KV114, KV124 and KV175 (7 pcs.) and Group 1 inclusions from KV103 and KV309 (7 pcs. not shown). Three additional samples of Group 1 inclusions were collected from the open pit. Compositions of olivine, clinopyroxene and chromite were measured using a JEOL JXA-8200 electron microprobe at the University of Oulu. Analytical conditions were 15 kV accelerating voltage, 30 nA beam current and peak and background counting times of 60 and 30 s, respectively. Under these conditions the detection limit for Ni is about 120 ppm and for Cr about 180 ppm. The accuracy of the analysis was monitored using olivine and chromite standards and relative errors are within ±2 % for major oxides (SiO_2, Al_2O_3, FeO, MgO, Cr_2O_3 and ±3 % for nickel. The built-in ZAF correction routine was used.

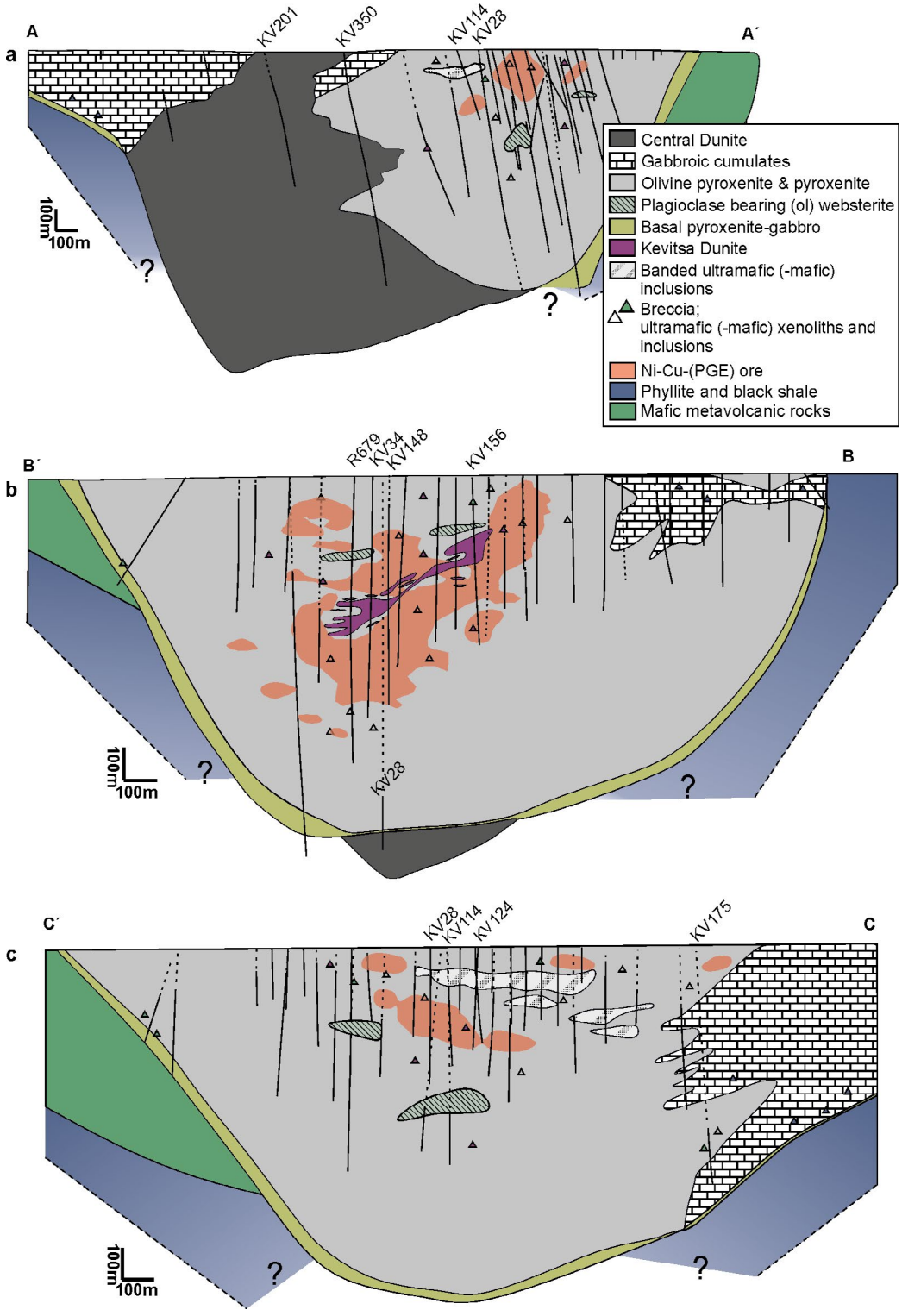

Figure 3. Cross sections (see Fig. 2) across the Kevitsa intrusion showing a) the Central Dunite, b) the Kevitsa Dunite and Central Dunite at the base of the intrusion, and c) the Group 2 slab-like banded ultramafic(-mafic) inclusion. “Breccia” refers to small scattered inclusions. The red area depicts the location of Ni-Cu-(PGE) ore. Sampled drill cores are labelled.

4. Field characteristics and petrographic descriptions of dunitic rocks

In this study, the dunitic rocks at Kevitsa are classified on the basis of their texture into two broad groups: i) dunitic cumulates (Fig. 4) and ii) recrystallized ultramafic inclusions (Figs. 5 and 6). The dunitic cumulates include the large Central Dunite body and Kevitsa Dunite. The latter occurs as large, locally 10s-m-thick inclusions within a cumulate sequence of olivine pyroxenites. The recrystallized ultramafic inclusions are further divided into two subgroups (Group 1 and 2) with differences in their spatial distribution within the Kevitsa intrusion and their texture, mineralogy and whole-rock compositions (particularly REE). The general features of these ultramafic rocks are described below. Additional photographs are provided in Electronic Appendix A.

4.1. Dunitic cumulates

4.1.1. Central Dunite

The modal mineralogy of the rocks forming the Central Dunite body range from dunite (most dominant) to wehrlite and feldspathic wehrlite but for simplicity, the term Central Dunite is adopted to refer to this body. The true dimensions of this body are unknown but recent drilling has shown it to be at least several hundred meters in thickness (Fig. 3a). The contacts between the Central Dunite and Kevitsa gabbros are altered and disturbed by quartz-chlorite-carbonate rocks that probably represent later veining at the contact. When clear, the contacts are sharp or sheared and locally seen to be brecciated by the Kevitsa pyroxenitic cumulates. At the base of the Kevitsa intrusion, the contact with the dunite in the footwall (Fig. 3b) is well defined and marginal series rocks (pyroxenite–gabbro) of the Kevitsa intrusion can be recognized, yet this sequence is thinner than that observed elsewhere in the intrusion.

4.1.2. Kevitsa Dunite

The Kevitsa Dunite comprises discrete irregular masses of cumulate-textured dunite, wehrlite (rarely lherzolite) and their feldspar-bearing variants (termed the Kevitsa Dunite for simplicity). It occurs in a N-S-trending zone at the core of the ore deposit as large raft-like lense(s) rather than a coherent intact layer (Fig. 3b). The contacts with its host olivine pyroxenites can be sharp but are usually irregular and complex (mingled). Also, the small brecciated clasts of Kevitsa Dunite are rounded, rather than blocky, and occasionally, seem to behave in a ductile way.

The Central and Kevitsa Dunites show similar textures and lithological variations (dunite, wehrlite, feldspathic wehrlite, Fig. 4) and are described together. The dunites (Figs. 4a and b) are composed of olivine (>90 %) and chromite (up to 5 %) and show adcumulate textures. In wehrlites, clinopyroxene (5–30 %) and rarely orthopyroxene occur as oikocrysts enclosing olivine and chromite, defining a poikilitic texture (Figs. 4c-f). Clinopyroxene (in dunites), plagioclase, primary phlogopite and amphibole (pargasite and edenite) occur as intercumulus phases. In wehrlites, the amount of intercumulus plagioclase may exceed 10 vol.% and the rocks are thus feldspathic (Figs. 4e and f). Accessory sulfides (mostly pyrrhotite) are rather common in the Kevitsa Dunite and Ni-Cu sulfides (regular ore) occur locally in association with mineralized olivine pyroxenites.

Olivine is typically subhedral and 0.5–3 mm in size with equilibrated grain boundaries. Slight deformation of the olivine grains is evidenced by kink bands and undulose extinction. Olivine chadacrysts are euhedral to rounded and fine grained (0.5–1 mm). Chromite occurs as equant to rounded inclusions in coexisting main silicate phases or as larger euhedral grains at grain boundaries. Clinopyroxene and orthopyroxene oikocrysts are large, up to 1 cm in size. Olivine is altered to serpentine and magnetite along cracks and pyroxenes to amphibole in variable degrees.

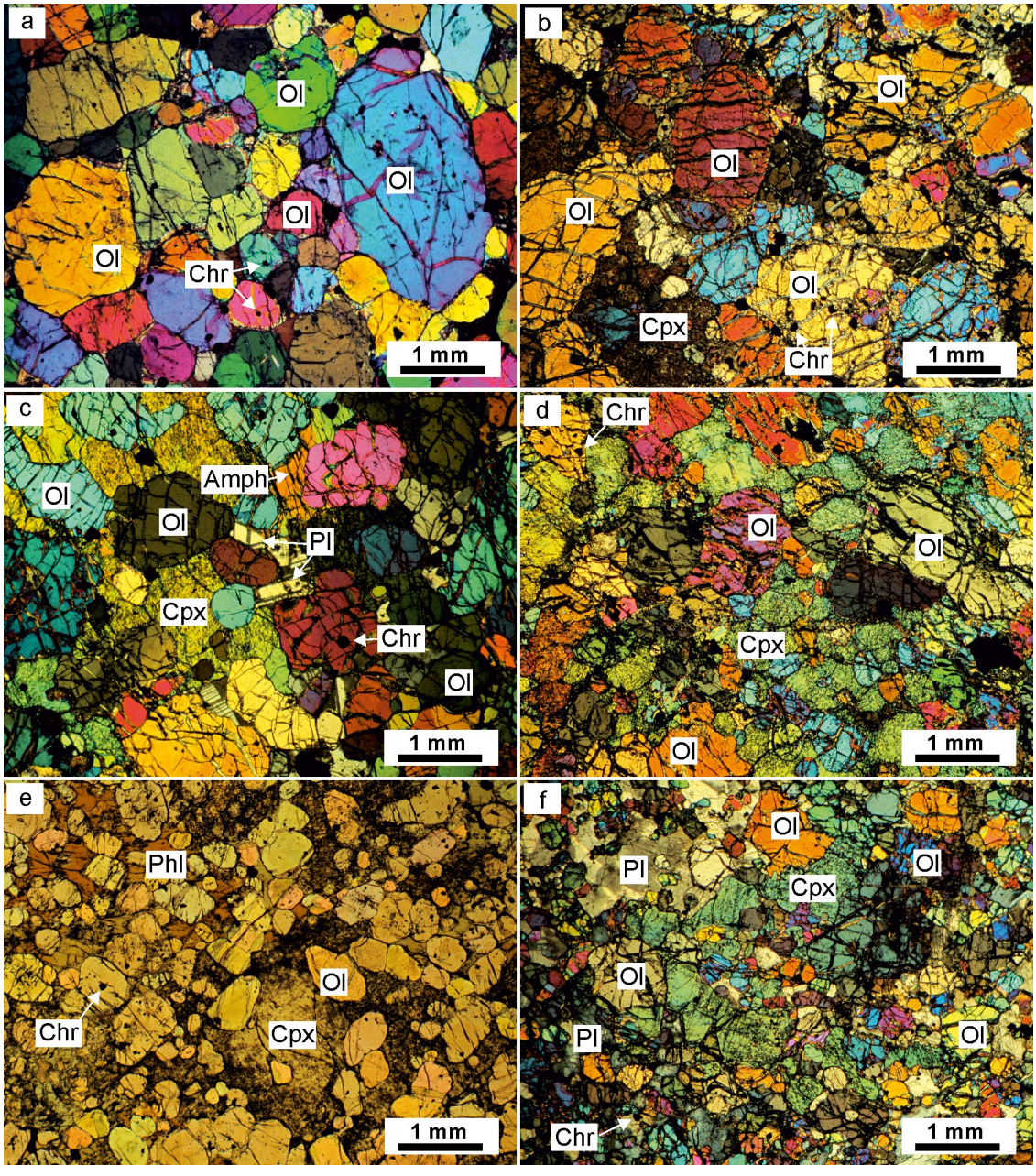

Figure 4. Photomicrographs of dunitic cumulates. a) Dunite adcumulate (Central Dunite); b) Moderately altered dunite adcumulate (Kevitsa Dunite); c) Wehrlite (Central Dunite); d) Wehrlite (Kevitsa Dunite). Single clinopyroxene oikocryst fills the entire picture; e) Wehrlite (feldspathic but all plagioclase altered to chlorite, not shown). Note the reduced olivine grain size (Central Dunite); f) Fine-grained feldspathic wehrlite (Kevitsa Dunite). Figures a-d and f taken with crossed polars and e with parallel polars. Ol = olivine, Cpx = clinopyroxene, Chr = chromite, Pl = plagioclase, Phl = phlogopite, Amph = amphibole.

Chlorite and/or sericite may replace plagioclase. At shallow levels, the Central Dunite is entirely serpentinized.

4.2. Recrystallized ultramafic inclusions

Common features of the recrystallized ultramafic inclusions are their fine grain size and granoblastic/interlobate (hornfelsic) texture (see Figs. 5 and 6), which distinguish them from the cumulate-textured variants. The inclusions range in size from millimeters to meters, most commonly being fist sized and smaller. The inclusions are most often rounded but may be irregular or angular in shape. Contacts with the host rocks are usually well defined.

4.2.1. Group 1

The Group 1 inclusions are olivine-clinopyroxene-chromite aggregates with trace sulfides in some samples (Fig. 5) and are denoted as breccia in Fig. 3. The polygonal olivine and clinopyroxene grains are small, varying in size from a few tens of micrometers to ~0.3 mm, rarely exceeding 0.5 mm. In some samples, the olivine grain size distribution is bimodal (Fig. 5b). Clinopyroxene may also occur as anhedral (interlobate) grains, enclosing olivine. Accessory chromite is found as rounded to equant inclusions in olivine and clinopyroxene and at grain boundaries.

Preferred orientation (Fig. 5a) and monomineralic stripes/bands of either olivine or clinopyroxene or both are observed in a few samples. Large relict olivine grains were only found in two samples (Fig. 5c); otherwise any primary textures are absent.

In general, sulfide-bearing inclusions are found hosted in mineralized rocks whereas inclusions within barren host rocks tend to be devoid of sulfides. The sulfides occur as fine disseminations in "interstitial" spaces between olivine and clinopyroxene, with the sulfide assemblages being similar to those in the host cumulate rocks. As proposed by Mutanen (1997), it is likely that sulfide liquid infiltrated into the inclusions during their recrystallization.

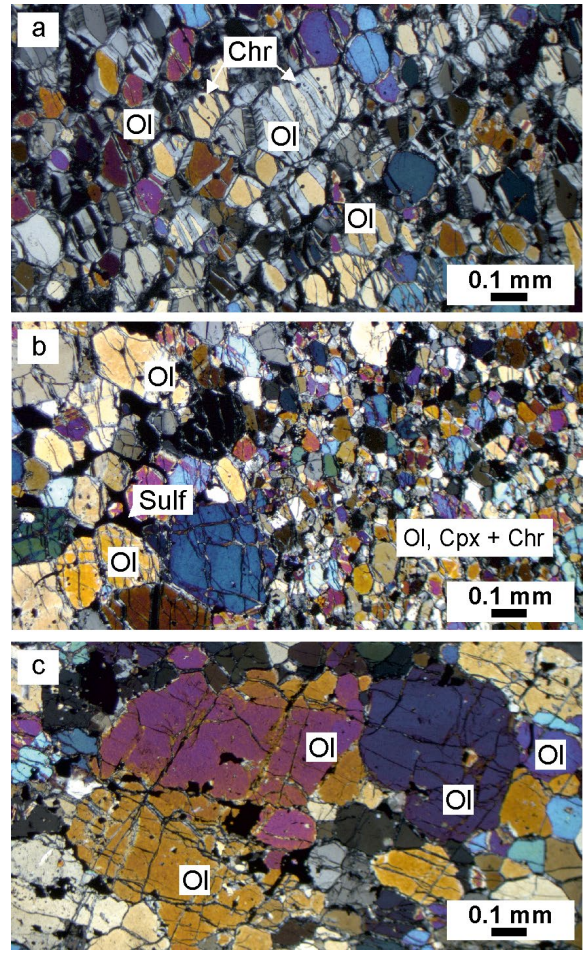

Figure 5. Photomicrographs of Group 1 recrystallized inclusions. a) Dunite inclusion with polygonal olivine showing preferred orientation and accessory chromite and clinopyroxene; b) Granoblastic wehrlite inclusion with a bimodal olivine grain size distribution. Note the sulfides (black) interstitial to the coarser-grained olivine on the left; c) Relict strained olivine porphyroclasts in a matrix of polygonal olivine and clinopyroxene. Crossed polars. Ol = olivine, Cpx = clinopyroxene, Chr = chromite, Sulf = sulfides.

4.2.2. Group 2

The Group 2 ultramafic inclusions are mineralogically diverse and consist in variable modes of olivine, clinopyroxene, orthopyroxene, and oxides with or without plagioclase, amphibole and sulfides (Fig. 6). A characteristic feature of the Group 2 inclusions is their banded nature, which is manifested by alternating dark olivine-dominated bands and

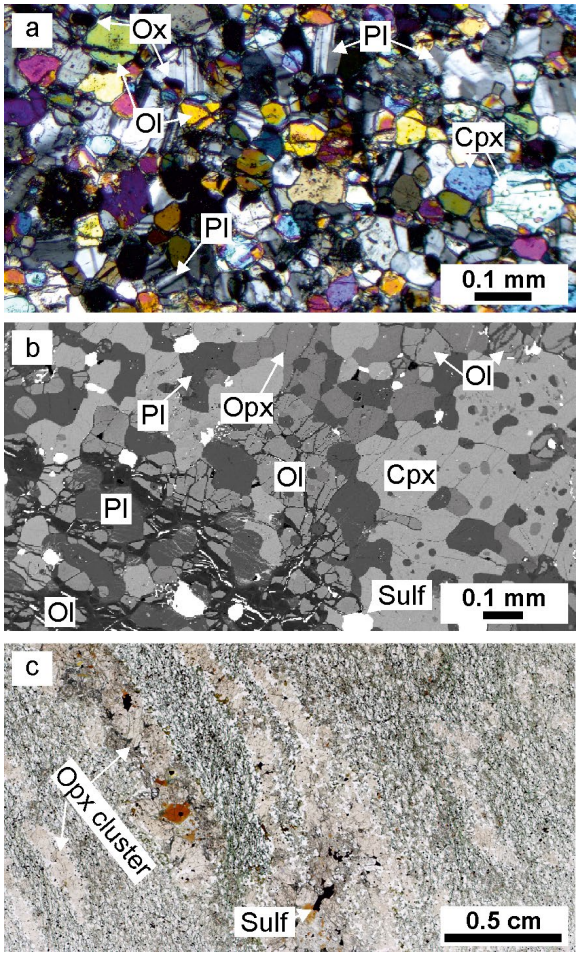

Figure 6. Textures of Group 2 inclusions. a) Photomicrograph of fine-grained, granoblastic olivine-clinopyroxene-orthopyroxene-plagioclase aggregate with accessory oxides. Crossed polars; b) Back-scattered electron image of the contact between plagioclase-pyroxene aggregate (up right) and olivine-dominated aggregate (down left). Note the minute inclusions of coexisting silicates. Bright minerals are sulfides and oxides; c) Scanned thin section image showing preferred orientation of orthopyroxene clusters (lineation) in a fine-grained matrix of olivine, clinopyroxene, plagioclase, orthopyroxene, oxides, and minor amphibole. Ol = olivine, Cpx = clinopyroxene, Opx = orthopyroxene, Pl = plagioclase, Ox = oxides, Sulf = sulfides.

lighter bands mainly composed of pyroxenes and plagioclase (Fig. 6b).

Olivine is always polygonal whereas pyroxenes and plagioclase can be irregular and anhedral (interlobate) (Figs. 6a and b). Oxides are enclosed in silicates or occur at grain boundaries and range in composition from chromite to magnetite and individual grains tend to be highly heterogeneous. Coexisting silicates and oxides are also found as microscopic inclusions in each other. Disseminated sulfides are present in some samples, but unlike in the case of the Group 1 inclusions, similar correlation with the presence of sulfidic inclusions in sulfidic host rocks is not observed. Foliation fabrics are rather common and in a few samples, preferred orientation of poikiloblastic orthopyroxene clusters define a weak lineation (Fig. 6c). Possible cataclastic deformation in one sample is recognized as parallel orientation of elongated, fine-grained olivine aggregates that show simultaneous extinction.

The occurrence of banded ultramafic inclusions is most prominent at shallow levels in the southern part of the intrusion where they occur as a more or less coherent slab (up to few tens of meters thick) that can be traced from south to north for more than 100 meters and even beyond that as a breccia zone (Fig. 3c). Rare mafic pyroxene-plagioclase (±minor olivine) hornfelses are found in association with Group 2 inclusions.

5. Mineral compositions

Chemical compositions of olivine, clinopyroxene and chromian spinel from the Central Dunite, Kevitsa Dunite, and Group 1 and Group 2 recrystallized inclusions are provided in Electronic Appendix B.

5.1. Central Dunite

The forsterite content of olivine in the Central Dunite ranges from 85.1 to 88.6 mol.%, being homogeneous within individual samples (Figs. 7a and b). The Ni content in olivine (2000–3500 ppm) broadly correlates with Fo but is variable in each sample (Fig. 7a). The MnO content ranges from 0.14 to 0.35 wt.% and correlate with Fo (Fig. 7b).

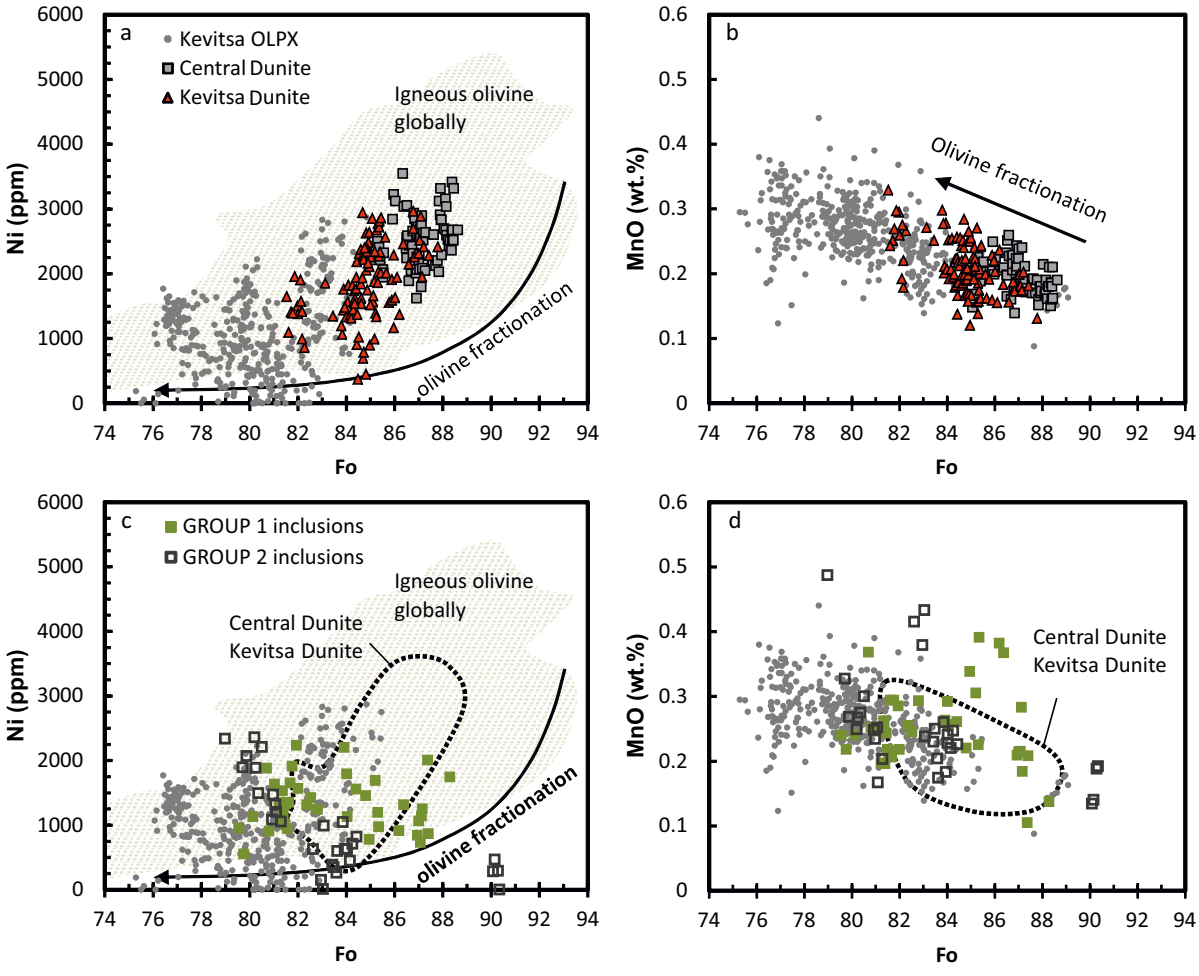

Figure 7. a) Fo (%) versus Ni (ppm) and b) Fo (%) versus MnO (wt.%) plots for olivine from the Central Dunite and Kevitsa Dunite and c) and d) for Group 1 and Group 2 inclusions, respectively Olivine compositions of Kevitsa olivine pyroxenites (OLPX) from unpublished data by the first author. Global olivine data from Sobolev et al. (2005), Straub et al. (2008, 2011), and Tamura et al. (2000) and the olivine fractionation line of Barberton komatiite after Tuff et al. (2005).

Chromite inclusions in olivine contain 30.1 to 40.9 wt.% Cr_2O_3 and 7.6 to 14.1 wt.% Al_2O_3 resulting in Cr# values [100*Cr/(Cr+Al)] between 77 and 64, and show TiO_2 contents of 0.4–2.5 wt.% (Figs. 8a and b). The chromites broadly fall in a primary magmatic chromite trend (Bliss & MacLean, 1975; Wang et al., 2005) on a Cr_2O_3 vs. Al_2O_3 diagram together with the chromite from Savukoski Group picritic volcanic rocks. In comparison to the chromite in komatiitic volcanic rocks, chromite in picrites and the Central Dunite is generally higher in TiO_2. The most primitive olivine and chromite compositions ($Fo_{>87}$ and ~40 wt.% Cr_2O_3 in chromite) were measured from the adcumulate dunites. The interstitial to oikocrystic clinopyroxene has Mg# [molar 100*Mg/(Mg+Fe)] of 87.1 to 90.7 and Cr_2O_3 contents up to 1.34 wt.% (Fig. 9).

5.2. Kevitsa Dunite

The forsterite content of olivine in the Kevitsa Dunite ranges from 83.9 to 87.4 mol.% (Figs. 7a and b), being homogeneous within individual samples, but Ni in olivine is more variable. As

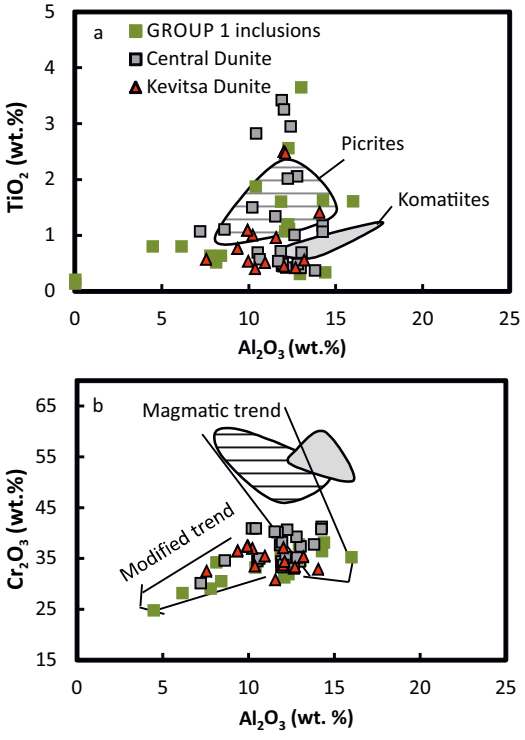

Figure 8. a) TiO_2 vs. Al_2O_3 and b) Cr_2O_3 vs. Al_2O_3 (b) plot for chromite from the Central Dunite, Kevitsa Dunite, and Group 1 inclusions. The magmatic chromite trend after Bliss and Maclean (1975) and the modified trend after Wang et al. (2005). Chromite compositions in picritic and komatiitic volcanic rocks (Savukoski Group) from Hanski and Kamenetsky (2013).

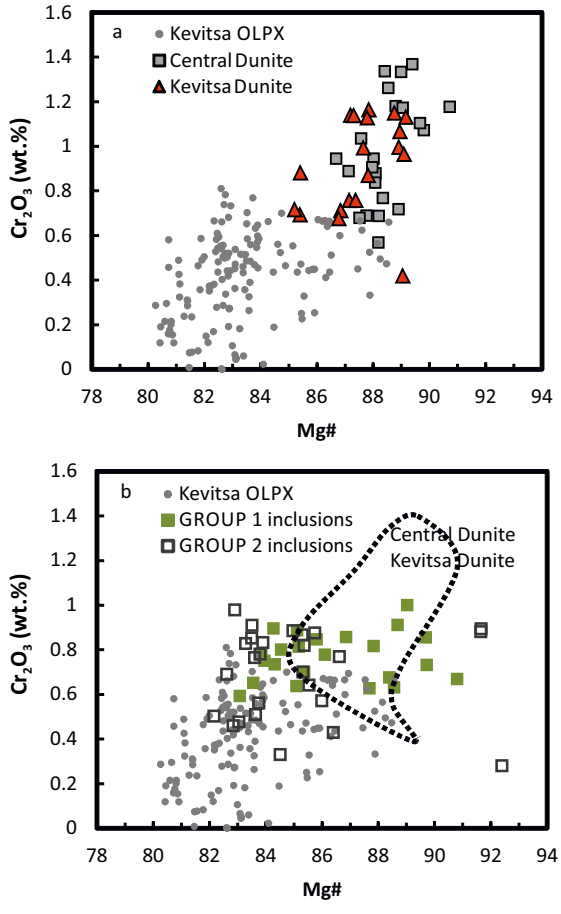

Figure 9. Cr_2O_3 (wt.%) vs. Mg# plot for clinopyroxene from the Central Dunite, Kevitsa Dunite, and Group 1 and Group 2 inclusions. Clinopyroxene compositions of Kevitsa olivine pyroxenites (OLPX) from unpublished data by the first author.

in the Central Dunite, the adcumulate dunites contain the most magnesian olivine ($Fo_{\sim 87}$) whereas wehrlites and feldspathic wehrlites show slightly more evolved compositions. Low Fo contents of ~82 mol.% were obtained from a separate fragment (1.5 m) of dunitic cumulate located a few tens of meters above the Kevitsa Dunite. The low Fo content probably reflects local equilibration with the host rock. Chromian spinel inclusions in olivine are compositionally similar to chromite in the Central Dunite (Fig. 8) but tend to contain slightly less Cr_2O_3 (32.5–37.4 wt.%, Cr# = 74–61). The TiO_2 concentration in chromite ranges from 0.5 to 2.5 wt.% and that of Al_2O_3 from 9.4 to 13.2 wt.%. Mg# of poikilitic clinopyroxene ranges from 85.4 to 89.1 and Cr_2O_3 from 0.68 to 1.16 wt.% (Fig. 9).

5.3. Group 1 inclusions

Recrystallized olivine in the Group 1 inclusions varies in composition from $Fo_{78.8}$ to $Fo_{88.3}$ and its Ni falls in the range of 550–2300 ppm and MnO between 0.11–0.39 wt.%, overlapping with the entire compositional range observed in dunitic cumulates and Kevitsa olivine pyroxenites (Figs. 7c and d). The forsterite and Ni contents do not exhibit any correlation. Within individual samples, the olivine composition may vary considerably (Fig. 10). The Mg# values of clinopyroxene vary between 83.1 and 90.8 (Fig. 9), being relatively variable

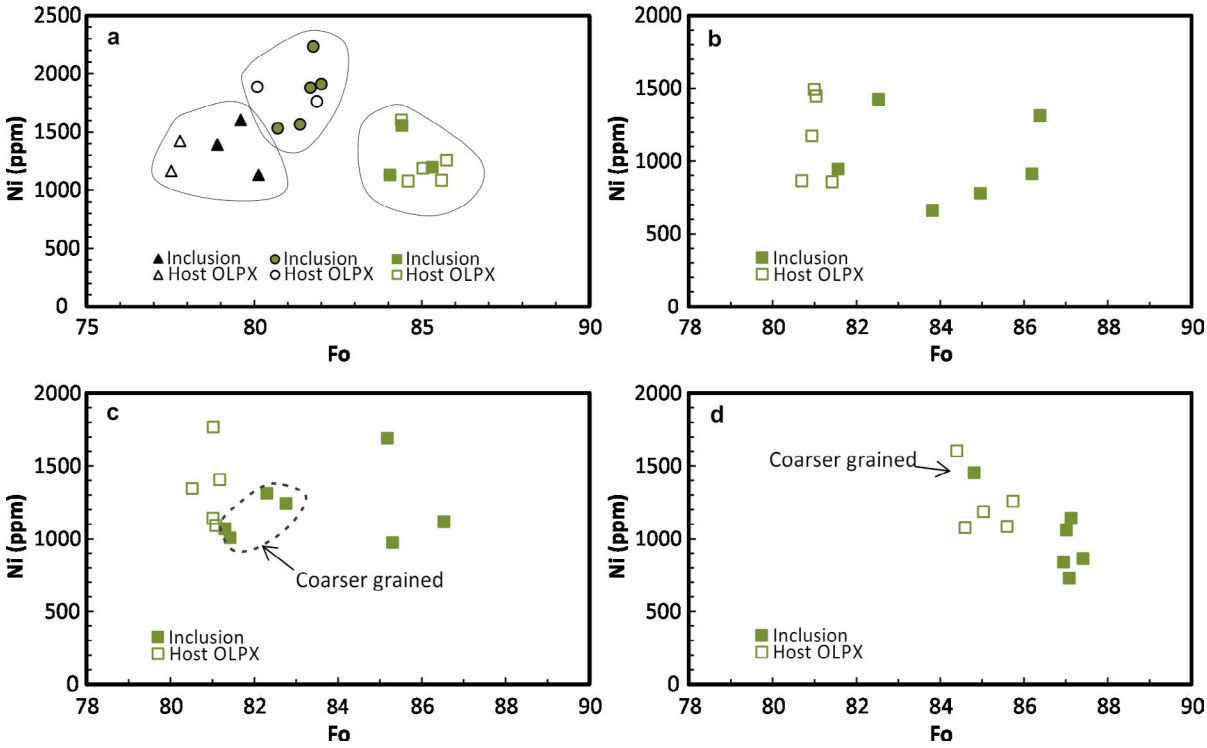

Figure 10. Examples of Ni and Fo contents of olivine in ultramafic inclusions and their host olivine pyroxenite (OLPX). a) Homogeneous olivine with similar Ni and Fo contents as olivine in the host rocks; b) Heterogeneous olivine population. Olivine compositions approach that of the host rocks; c) and d) Inclusions with a bimodal olivine grain size distribution. The composition of the coarser-grained olivine mimics that of the olivine in the host rock.

within individual samples. The Cr_2O_3 content in clinopyroxene is relatively high (0.59 to 1.0 wt.%), yet correlation with Mg# is poor.

The compositions of olivine in the inclusions and their immediate host olivine pyroxenite are usually very similar (Figs. 10a and b, data tabulated in Electronic Appendix B). In a few samples, in which the polygonal olivine is bimodal in its size distribution, the larger olivine grains found at/near the contact are compositionally identical to the olivine in the host rock whereas the fine olivine grains can be more forsteritic (Figs. 10c and d). It is concluded that such features were accomplished by equilibration of silicates under slowly cooling conditions. Similar adjustment of olivine compositions has been documented at contacts between mantle peridotite xenoliths and their host lavas (Klügel, 1998).

Spinel in the Group 1 inclusions varies compositionally from chromite to chromian magnetite. Cr_2O_3 (28.1 to 38.1 wt.%) and Al_2O_3 (4.5 to 16 wt.%) show a positive correlation, suggesting some modification of the primary igneous chromite (cf. Wang et al., 2005) during and/or prior to recrystallization if a common protolith is assumed. The majority of the analyzed chromite grains in the Group 1 inclusions, however, can be considered to have retained their primary igneous compositions and are identical to the chromite in the dunitic cumulates.

5.4. Group 2 inclusions

The forsterite content of olivine in the Group 2 inclusions falls dominantly into a range of 79.9 to 84.4 mol.% (Figs. 7c and d). One sample showed a

higher Fo of ~90 mol.%. The Ni content correlates negatively with Fo (Fig. 7c). The Mg# value of clinopyroxene ranges from 82.2 to 86.6 (~92 in the sample with highly forsteritic olivine) and the Cr_2O_3 content varies from 0.33 to 0.89 wt.%. Due to the obvious grain-scale heterogeneities of the oxide phases in the Group 2 inclusions, they are excluded from the discussion.

6. Whole-rock chemistry

Representative whole-rock compositions for the Central Dunite, Kevitsa Dunite and Group 1 and Group 2 recrystallized inclusions are provided in Electronic Appendix C. Loss of ignition (LOI) values range from zero to more than 10 wt.%, reflecting variable degrees of serpentinization of the rocks. In the following descriptions, the analytical data are calculated volatile-free.

6.1. Central Dunite

The unaltered adcumulate dunites in the Central Dunite have high MgO contents up to ~44 wt.% and Cr contents of 5200–5500 ppm and they record very low concentrations of TiO_2 (~0.1 wt.%), Al_2O_3 (~1.4 wt.%), CaO (~1.2 wt.%), Na_2O (<0.4 wt.%), and Y (<2.3 ppm) (Fig. 11), consistent with the adcumulate nature of the rocks. The transition from dunite to wehrlite and the appearance of oikocrystic Ca-pyroxene and increasing contents of intercumulus plagioclase are reflected by decreasing MgO (<40 wt.%) and increasing CaO (~3–7 wt.%) and Al_2O_3 (~2–6 wt.%). Feldspathic wehrlites are most aluminous. Chromium also decreases systematically with falling MgO. Chondrite-normalized REE patterns for rocks from the Central Dunite are mildly enriched in LREE (Ce_N/Yb_N = 1.4–2.0) and comparable to the patterns of typical Kevitsa olivine pyroxenites (Fig. 12a).

6.2. Kevitsa Dunite

The MgO content in the Kevitsa Dunite rocks ranges from 31 to 41 wt.% (Fig. 11), with the majority of the values falling below 38 wt.%. The CaO content is mostly higher than 3 wt.%, consistent with the presence of clinopyroxene oikocrysts. The whole-rock major element compositions mainly overlap with those of the wehrlites and feldspathic wehrlites in the Central Dunite. The four samples from the Kevitsa Dunite analyzed for rare earth elements show variable REE characteristics (Fig. 12b). Two of the samples have fairly flat REE patterns (Ce_N/Yb_N ~1.5) and positive Eu anomalies. One sample shows a negative Eu anomaly and Ce_N/Yb_N below 1.0 and one has a distinct LREE enrichment relative to HREE (Ce_N/Yb_N ~2.7).

6.3. Group 1 inclusions

The Group 1 inclusions have high MgO (29–39 wt.%) and Cr (1900–4400 ppm) contents and low incompatible trace element contents (Fig. 13), having an overlapping composition with dunitic cumulates. The Al_2O_3 content is very low (<1.5 wt.%), reflecting the lack of plagioclase in these rocks. The total iron content (FeO_T) varies widely (9–18 wt.%) but is not related to the presence of sulfides. Chondrite-normalized REE patterns mimic those seen in the host Kevitsa olivine pyroxenites (Fig. 12c). Notably, one of the LREE-enriched inclusions is hosted by LREE-enriched (Ni-PGE ore type) olivine pyroxenite. The other LREE-enriched sample is a boulder collected from the open pit and thus such a relationship cannot be determined.

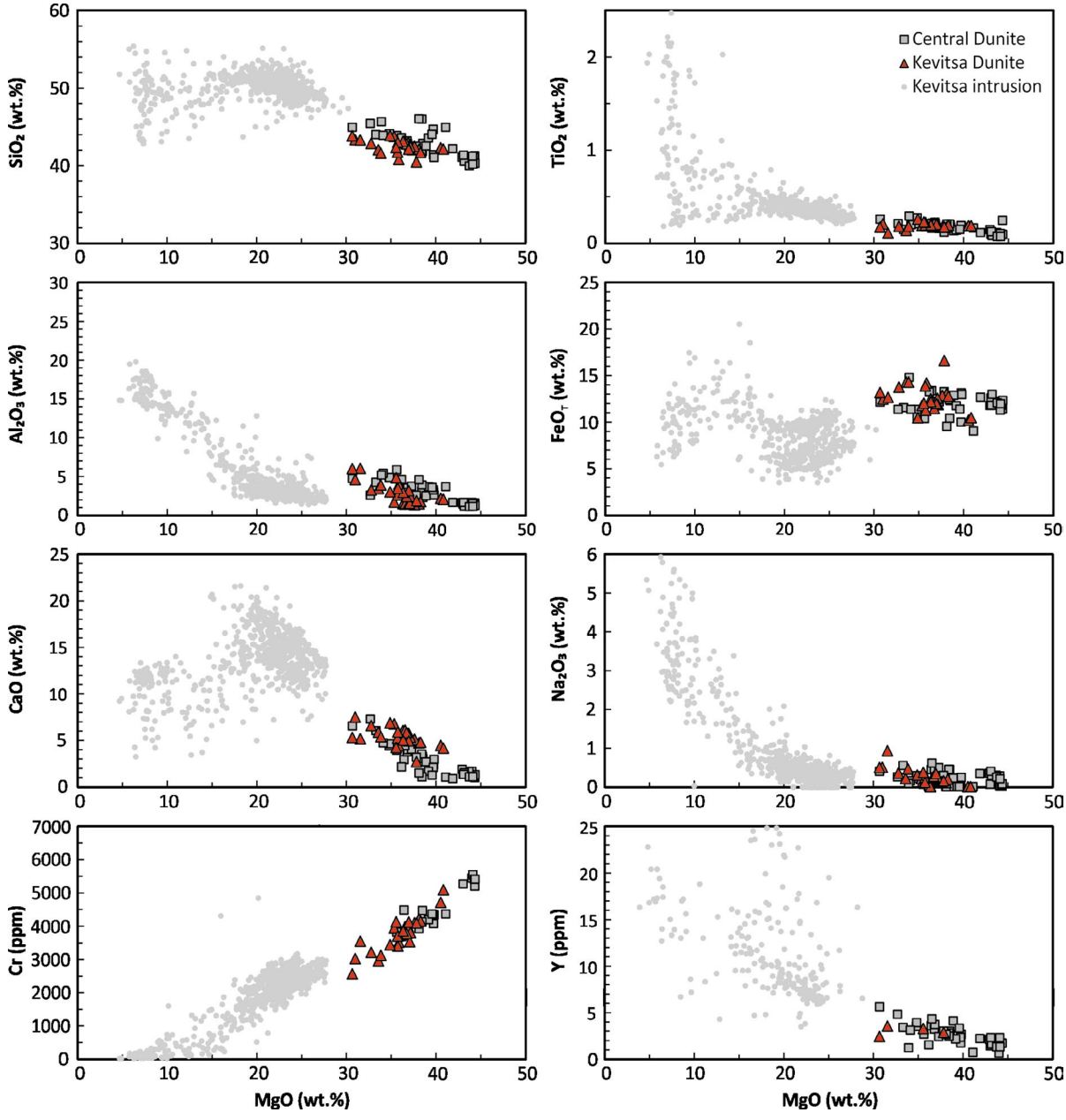

Figure 11. Variation of major element oxides, Cr and Y as a function of MgO in Central Dunite and Kevitsa Dunite rocks and Kevitsa mafic and ultramafic cumulate rocks.

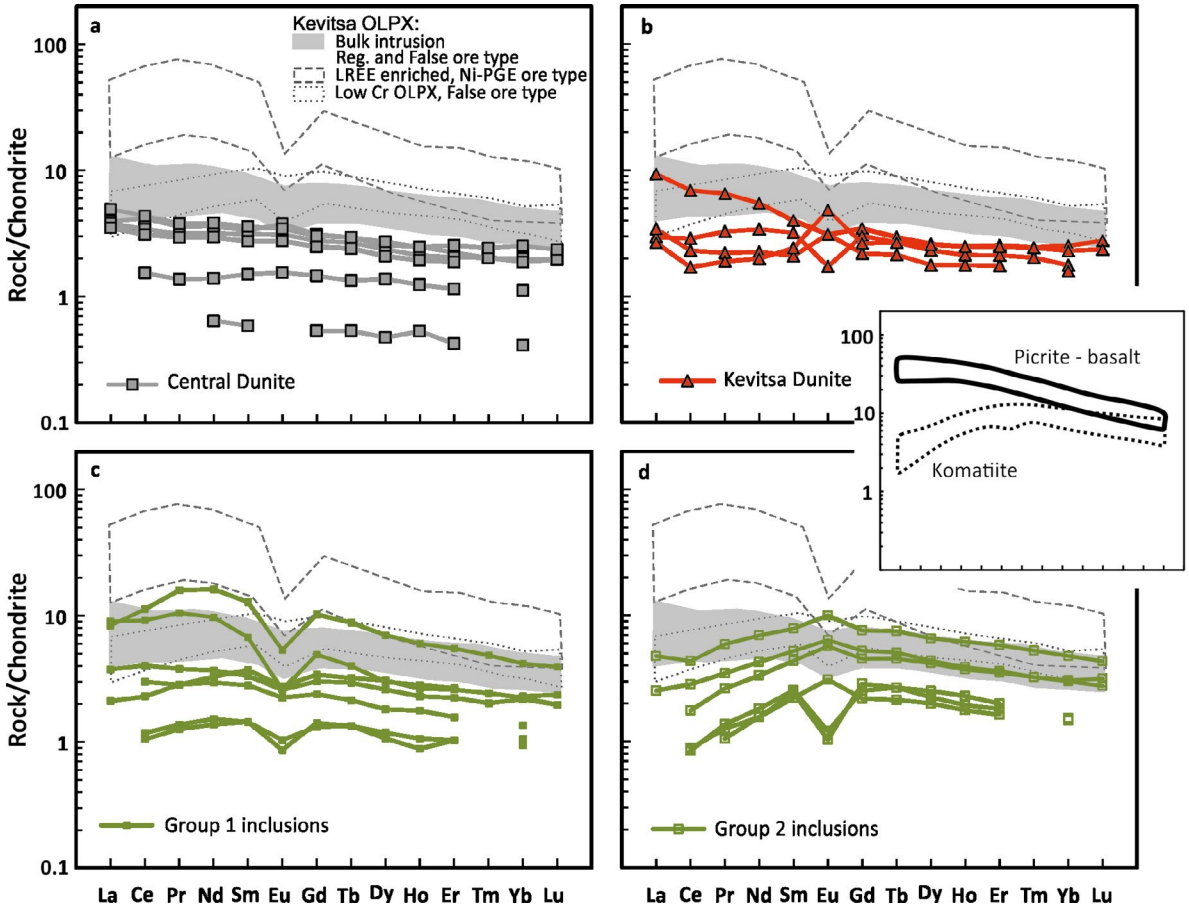

Figure 12. Chondrite-normalized rare earth element (REE) patterns for Central Dunite rocks (a), Kevitsa Dunite rocks (b), Group 1 inclusions (c), and Group 2 inclusions (d). The REE patterns for Kevitsa olivine pyroxenites are from Hanski et al. (1997) accompanied by mine data and the REE patterns for komatiitic and picritic rocks (Savukoski Group) from Hanski et al. (2001). Normalizing values are from Sun and McDonough (1989).

6.4. Group 2 inclusions

The MgO content of the Group 2 inclusions ranges from 20 to 37 wt.% (Fig. 13). The concentrations of Al_2O_3, CaO and TiO_2 increase systematically with falling MgO, whereas that of Cr decreases. FeO_T is variable (9–19 wt.%) and not related to the presence of sulfides. The compositions of Group 2 inclusions broadly fall on igneous trends defined by the Savukoski Group 2.06 Ga komatiitic volcanic rocks (Hanski et al., 2001) and ultramafic metavolcanic country rocks of the Kevitsa intrusion.

The Group 2 inclusions show hump-shaped chondrite-normalized REE patterns (Fig. 12d) with LREE depletion relative to HREE (Ce_N/Yb_N = 0.6–0.9). The two samples with a distinct negative Eu anomaly represent bands with low contents of plagioclase (Al_2O_3 <3 wt.%). In terms of their REE characteristics, the Group 2 inclusions are comparable to the 2.06 Ga komatiitic volcanic rocks (Hanski et al., 2001).

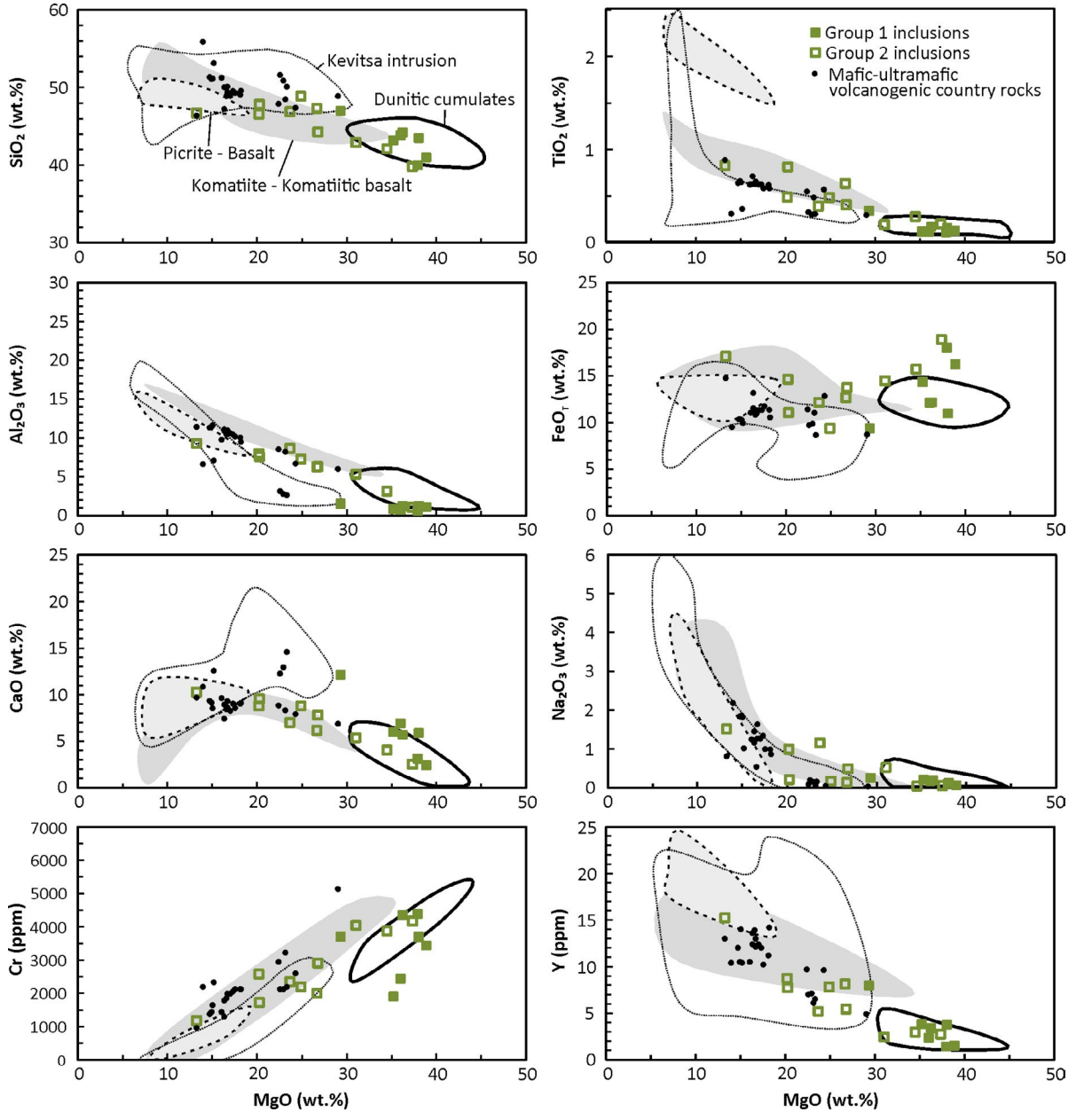

Figure 13. Variation of major element oxides, Cr and Y as a function of MgO in Group 1 and Group 2 inclusions. The fields for dunitic cumulates (Central Dunite and Kevitsa Dunite) and Kevitsa intrusion taken from Fig. 11 and the fields for 2.06 Ga komatiitic and picritic rocks (Savukoski Group) from Hanski et al., (2001).

7. Discussion

7.1. Cogenetic magmatic origin of the Central and Kevitsa Dunites

Within crustal magma chambers, dunite may form by primary magmatic (cumulate) processes from magnesian parental magmas (e.g., Raedeke & McCallum, 1984; Chai & Naldrett, 1992). Alternatively, magmatic infiltration and replacement may account for dunite formation at the expense of other ultramafic lithologies (e.g., Irvine, 1980; Raedeke & McCallum, 1984). Regarding the origin of discordant magnesian dunite pipes at Bushveld, Scoon & Mitchell (2004) argued against replacement origin based on the observation that the mineral compositions in the dunites are more primitive than in their wall rocks. Analogously, the mineral compositions in the Central and Kevitsa Dunites are more primitive than in the Kevitsa olivine pyroxenites (Figs. 7 and 9). Also, the dunites contain abundant chromian spinel that is only a rare phase in the Kevitsa cumulates, although some chromium could have been dissolved from clinopyroxene. Moreover, the lack of sufficient amounts of orthopyroxene in any of the Kevitsa rocks precludes the possibility of replacement of orthopyroxene by olivine, a process suggested to have formed the platiniferrous dunite pipes of the Bushveld Complex (Schiffries, 1982; Stumpfl & Rucklidge, 1982) and discordant dunite bodies at Stillwater (Raedeke & McCallum, 1984). The mineral compositional trends and correlations of Fo with MnO and NiO in olivine and Mg and Cr_2O_3 in clinopyroxene are consistent with crystal fractionation.

The overall discordant geometry of the Central Dunite (see Fig. 3a) with respect to the Kevitsa intrusive succession together with the intrusive contact relations suggests that the Kevitsa intrusive succession and the Central Dunite formed as a result of different magmatic events. Although the Central Dunite looks like a cross-cutting plug in surface geological maps and cross sections (see Figs. 2 and 3a), the contact relationships suggest that it predates the Kevitsa mafic-ultramafic successions. This interpretation is consistent with Mutanen (1997) who considered the Central Dunite to be a large roof pendant xenolith.

In the view of the large size of the Kevitsa Dunite body and the commonly irregular contacts with its host olivine pyroxenites, in addition to the preliminary "komatiitic xenolith" model (Mutanen, 1997), some alternative interpretations can be considered for the genesis of the Kevitsa Dunite. For instance, Li & Naldrett (1999) regarded irregular inclusions of peridotite in the Voisey´s Bay intrusion as fragments of early cumulates brecciated by later magma emplacements. Similar inclusion-host rock relations have been reported by Bushey et al. (2006) from the Bear Mountain intrusive complex with a complex multistage magmatic history. The peridotite sills within the Rum layered complex (Bèdard et al., 1988), Honningsvåg intrusive suite (Tegner & Robins, 1996) and Kap Edvard Holm intrusion (Tegner & Wilson, 1993), and the dunite pipes at Bushveld (Scoon & Mitchell, 2004, 2009) are considered to originate by intrusion of relatively late mafic/ultramafic magmas into adjacent semi-consolidated cumulates. The Duke Island igneous complex, which contains a younger dunite-peridotite core enveloped by older mafic-ultramafic cumulates (Irvine, 1974), and the Fongen-Hyllingen complex, in which a late peridotite–troctolite body transects an older layered gabbro (Sørensen & Wilson, 1996), are examples that are interpreted as two-phase intrusive suites, yet with a considerable time span between the magma emplacements. In all these cases, discordant (with respect to magmatic layering) and/or intrusive contact relations are identified.

The irregular shape and complex contact zones of the Kevitsa Dunite could possibly be explained by late-stage intrusion of Mg-rich magma into semi-consolidated Kevitsa olivine pyroxenites. A problem arising from a late intrusion hypothesis is the lack of any rock lithologies that could be interpreted as the residual magma or rock reacted with this residual left after extraction of olivine and chromite from the

melt. Secondly, the Kevitsa Dunite could represent the most primitive phase of the Kevitsa cumulate sequence but became invaded and disrupted by later magma injections.

The whole-rock and mineral compositional data from the Kevitsa Dunite slightly overlap those of the Kevitsa olivine–pyroxene cumulates with highest MgO (Fig. 11), Fo (Fig. 7) and Mg# (Fig. 9). However, on the basis of the analogous cumulate mineralogy, texture and compositional characteristics, the Kevitsa Dunite is more comparable to the Central Dunite, strongly implying a cogenetic relationship between the two. Consequently, it is concluded that the Kevitsa Dunite represents a large, ruptured "slice" of the Central Dunite that got trapped within the later-invading Kevitsa magma. The dunites at the base of the Kevitsa intrusion are entirely composed of tight adcumulates and hence, the Kevitsa Dunite, which records slightly more evolved mineral compositions and is rather rich in poikilitic clinopyroxene in comparison to the overall range seen in the Central Dunite, could represent a "missing" part of that dunitic cumulate sequence.

7.2. Parental magma for dunitic cumulates

The precise composition of the parental liquid is difficult to assess on the basis of cumulates. However, some conclusions can be drawn from the presented data. The Fo content of olivine is related to the MgO/FeO ratio of the magma from which it crystallized. Using the olivine-melt Mg-Fe exchange coefficient of 0.30 (Roeder & Emslie, 1970), the most primitive olivine in the Central Dunite ($Fo_{88.6}$) is in equilibrium with a melt with MgO/FeO of 1.31. It can be noted that the corresponding MgO/FeO value for the magma of the Kevitsa olivine pyroxenites is 0.99 based on the most Mg-rich olivine with $Fo_{85.4}$ (unpublished data by the first author). Compositional modification of the olivine due to the trapped liquid effect (Barnes, 1986) is assumed to be insignificant in both cases.

The magma forming the Central Dunite (and the Kevitsa Dunite) must have been relatively rich in MgO (at least 10 wt.%) to crystallize extensive dunite with a relatively high forsterite ($Fo_{88.6\text{-}84.0}$) content. The similar REE characteristics of the Savukoski Group picritic volcanic rocks and the Central Dunite suggest that the dunitic rocks represent cumulate parts (conduits) of the former. Hanski et al. (2001) showed that the Savukoski Group komatiitic and picritic volcanic rocks are distinctly different in their REE characteristics (see Fig. 13) but record rather similar initial ε_{Nd} values (+2 to +4). Hanski & Kamenetsky (2013) also noted a difference in chromite and chromite-hosted melt inclusion compositions between these volcanic rocks. The compositional features of chromite (e.g., Al_2O_3/TiO_2) from the Central Dunite are more close to those from picrites than komatiites.

7.3. Interactions between the Kevitsa Dunite and Kevitsa magma

Melting of Fo-rich olivine in the Kevitsa Dunite by the Kevitsa magma is unlikely, but mechanical disaggregation may have taken place. The interstitial plagioclase and any hydrous phases, however, were likely subjected to melting. Mobilization of low-temperature phases at the contact zones may have led to disintegration of the cumulus framework of the Kevitsa Dunite, provoking disaggregation of olivine and resulting in complex (mingled) contact zones observed against Kevitsa olivine-pyroxene cumulates. Primary amphibole and phlogopite are less common in the Kevitsa Dunite compared to the Central Dunite, supporting a loss of hydrous phases from the Kevitsa Dunite. Late-stage sulfides may have replaced intercumulus phases in the Kevitsa Dunite, explaining the similar sulfide assemblages of the Kevitsa Dunites and their olivine pyroxenite host rocks. Local equilibration between the silicate phases within the Kevitsa Dunite and its host olivine pyroxenites may have occurred by diffusional exchange. The dominantly much higher Cr contents in clinopyroxene and

Fo in olivine in the Kevitsa Dunite compared to the Kevitsa olivine pyroxenites, however, do not support comprehensive influence of the Kevitsa silicate liquids on the composition of the Kevitsa Dunite, i.e. interaction by the process of magmatic infiltration metasomatism (cf. Irvine, 1980).

The REE patterns in the Kevitsa Dunite vary considerably and differ from the REE characteristics observed in the Central Dunite and the Kevitsa ultramafic cumulates. The different REE patterns, however, are observed even in samples collected from the same drill core intersection of intact Kevitsa Dunite. Regardless of the genetic relations of the Kevitsa Dunite either to the Central Dunite or Kevitsa olivine pyroxenite cumulates, the variations in REE characteristics in the Kevitsa Dunite are presumably a result of interaction with the Kevitsa magma. The observed Eu anomalies in the Kevitsa Dunite can be related to the presence of plagioclase in these samples; negative Eu anomalies are measured from Kevitsa Dunite devoid of plagioclase (Al_2O_3 = 1.6 wt.%) whereas positive Eu anomalies are observed in feldspathic wehrlites (Al_2O_3 ~5 wt.%). The samples of the Central Dunite analyzed for REEs are dunites and wehrlites with Al_2O_3 of ~3 wt.% or less and hence, in terms of the modal mineralogy, not fully comparable to the analyzed samples of the Kevitsa Dunite. A slight positive Eu anomaly can be observed in the Central Dunite richest in intercumulus plagioclase. Although alteration may account for some of the REE distribution in the Kevitsa Dunite, the negative Eu anomaly probably indicates loss of intercumulus plagioclase. To generate the high LREE content in one of the samples of the Kevitsa Dunite, a more pronounced reaction with the Kevitsa magma is required. Olivine in this sample shows a Fo content of ~84.5 mol.% and clinopyroxene has Mg# of ~87 and Cr_2O_3 of 0.7 wt.%. These are among the most evolved compositions measured from the Kevitsa Dunite and modification by an additional clinopyroxene component of the Kevitsa magma, probably related to the Ni-PGE ore type magma, may account for the observed LREE enrichment.

7.4. Relationship between the dunitic cumulates and Kevitsa olivine-pyroxene cumulates

The most apparent difference between the Kevitsa pyroxenitic cumulates and the dunitic cumulates is the more primitive nature of the latter as evidenced by the liquidus mineral assemblage and whole-rock and mineral compositions. Nevertheless, a number of similarities exist, including: 1) Whole-rock major and trace elements (except Al_2O_3, Fig. 11) and mineral compositions fall on the same linear trends on the MnO and NiO vs. Fo diagrams for olivine (Fig. 7) and the Cr_2O_3 vs. Mg# diagram for clinopyroxene (Fig. 9). 2) Pyroxene is mainly clinopyroxene rather than orthopyroxene. 3) Clinopyroxene in both rock types is characterized by low Al_2O_3 and TiO_2 contents (<2.5 and <0.6 wt.%, respectively, in clinopyroxene in Kevitsa olivine pyroxenites; unpublished data by the author). Although the low Al and Ti contents in clinopyroxene may solely reflect crystallization at a low pressure, it may additionally suggest crystallization from similar magma types. 4) Both rock types record a considerable variation in olivine Ni at constant Fo. Some variation in olivine compositions in the ore-bearing rocks may arise due to Ni-Fe exchange with sulfides (Li & Naldrett, 1999) but cannot alone explain the observed variations. 5) The REE patterns in the Central Dunite are comparable to those of the bulk Kevitsa intrusion. 6) Both rocks are relatively hydrous. The presence of primary hydrous phases in the Kevitsa ultramafic rocks is often overprinted by alteration and hence the original abundance of amphibole/phlogopite is hard to discern. Nevertheless, relatively abundant pegmatoidal dykes and pockets suggest hydrous conditions. The hydrous nature of the Kevitsa magma may also explain the low plagioclase content in the Kevitsa olivine pyroxenites as the stability of plagioclase decreases at elevated P_{H2O} (e.g.,Feig. et al., 2006; Howard et al., 2013). The high water content of the Kevitsa magma, however, may have been obtained by

assimilation of the country rocks and dehydration reactions (discussed below).

Their close spatial relationship together with the similarities mentioned above indicates that the dunitic cumulates and the Kevitsa intrusive succession may well have crystallized from genetically related magmas at differing stages of evolution.

7.5. Origin of the recrystallized ultramafic inclusions

The fine grain size and granoblastic textures are common features for both Group 1 and Group 2 inclusions, indicative for thermal metamorphism and textural readjustment. The presented data and observations are used to assess the character of the protoliths for the two types of recrystallized inclusions and to discuss their origin, yet this is not straightforward due to the lack of any well-recognizable primary textures and potential chemical modifications accompanying the thermal metamorphism.

7.5.1. Group 1 inclusions

In terms of whole-rock compositions, the Group 1 inclusions show a geochemical affinity towards the dunitic cumulates and particularly towards their clinopyroxene-rich variants (wehrlites). The REE characteristics, on the other hand, mimic those observed in Kevitsa ultramafic rocks, though few samples record REE abundances typical for the dunitic cumulates. The olivine and clinopyroxene compositions show a fairly wide variation and overlap the range seen in both dunitic cumulates and Kevitsa olivine pyroxenites. However, the mineral chemical data obtained from the inclusions and their immediate host rocks suggest that the compositions of olivine and clinopyroxene were adjusted with their surroundings. Consequently, it is reasonable to assume that REEs were also equilibrated. This is likely at least for the LREE-enriched inclusion found in association with LREE-enriched olivine pyroxenite. The presence of chromian spinel is a characteristic feature for Group 1 inclusions and dunitic cumulates and their identical magmatic compositions provide the most convincing evidence for the relationship of the two. This is supported by the common occurrence of Group 1 inclusions (although not exclusively) in close association with the Kevitsa Dunite and the presence of larger olivine crystals and clinopyroxene oikocrysts in some samples, which are interpreted as preserved primary crystals. The anhydrous mineralogy of the Group 1 inclusions can potentially be explained by partial melting and loss of any easily fusible minerals (e.g., plagioclase). Partial melting of the low-temperature phases would evidently increase the porosity of the inclusions and probably enabled sulfide liquid to infiltrate into them.

On the basis of textures and mineral compositions, the origin of olivine (and clinopyroxene) is hard to constrain. Metamorphic olivine may form through deserpentinization reactions of altered ultramafic precursors. Such an olivine is generally high in Fo (>>90 wt.%) and often also MnO (>1 wt.%) and commonly contains magnetite inclusions formed from liberated excess iron (Arai, 1975; Vance & Dungan, 1977; Nozaka & Shibata, 1995; Nozaka, 2010; Khedr & Arai, 2012). Although scattered oxide inclusions other than Cr-spinel may occur within the recrystallized olivine grains, they probably are related to a late-stage breakdown of both clinopyroxene and olivine to secondary magnetite, which is commonly observed in the Kevitsa olivine pyroxenites. None of the analyzed olivine grains ($Fo_{78.8-88.3}$) are particularly rich in Fo but few grains record elevated MnO contents with respect to the igneous fractionation trend defined by the dunitic cumulates and Kevitsa olivine pyroxenites (Fig. 7d). Dehydration of serpentinites or chlorite- and amphibole-bearing serpentinites produces mineral assemblages of olivine, orthopyroxene and Cr-Fe spinel, which are stable at high temperatures. Notably, the Group 1 inclusions entirely lack orthopyroxene.

Dynamic recrystallization (deformation induced) may provoke crystallization of primary olivine to fine-grained neoblasts (e.g., Mercier & Nicola, 1974; Paktunc, 1984; Rehfeldt et al., 2007). The compositions of the olivine neoblasts reflect the compositions of the primary olivine crystals. The preferred orientations, relict strained olivine and monomineralic bands indicate that strain and stress may well have accompanied recrystallization, facilitating development of neoblastic olivine. However, there is no systematic correlation between Ni and Fo in olivine nor between Cr_2O_3 and Mg# in clinopyroxene, which would be expected assuming the olivine grains in the Group 1 inclusions represent neoblasts of the olivine of the dunitic cumulates. Aside from the compositional modification due to equilibration with the host rocks, the presence of sulfide phases in some of the inclusions may account for some inconsistency in the Ni_{OL}-Fo relations due to Fe-Ni exchange (Li & Naldrett, 1999). Variable Ni_{OL}-Fo relations, distinct from what is expected for igneous olivine, are not uncommon for metamorphic olivine in metamorphosed ultramafic rocks. For example, Nozaka (2003) reported sample-scale compositionally heterogeneities in olivine crystals in thermally metamorphosed serpentinites from Southwest Japan and suggest that they are due to intermingling of relict primary olivine grains with metamorphic secondary olivine and compositional variation within the metamorphic olivine themselves. The olivine in Group 1 inclusions may represent a mixture of neoblastic and metamorphic olivine aside sparse relict grains. The mineral compositions are further modified by the presence of sulfides, compositional equilibration and diffusional exchange with the host rocks. Also, metasomatic growth could explain the observed grain size coarsening at the margins of inclusions accompanied by mineral compositional changes towards the compositions in host rocks.

We cannot rule out the possibility that the Group 1 inclusions originate from some altered peridotite, other than the dunitic cumulates described herein. Assuming that the REE abundances of the Group 1 inclusions were modified along with mineral compositions, the distinct REE characteristics of the Group 1 and Group 2 inclusions do not exclusively rule out the potential genetic relationship of the two.

7.5.2. Group 2 inclusions

The Group 2 inclusions show hump-shaped REE patterns, which are similar to those of the Savukoski Group komatiitic volcanic rocks in the area. The REE patterns suggest that the REE abundances were not affected by thermal metamorphism, metasomatism, alteration or reactions with the enclosing Kevitsa magma. It is concluded that the Group 2 inclusions are xenoliths of adjacent country rocks and most likely komatiitic in origin.

The mineral assemblage of the Group 2 inclusions, containing olivine, clinopyroxene, orthopyroxene, oxides ± plagioclase, amphibole, and sulfides in variable proportions, is in line with derivation through dehydration and high-temperature recrystallization of altered ultramafic precursors (e.g., Springer, 1974; Ashley et al., 1979). Nickel in olivine correlates negatively with Fo, which is not unusual for metamorphic olivine derived by dehydration of serpentine (Kunugiza, 1980; Säntti et al., 2006) or chlorite (Peltonen, 1990). Kunugiza (1980) regarded the negative correlation as a reflection of the degree of consumption of magnetite during serpentine dehydration as Fe and Ni are concentrated in magnetite rather than in serpentine. Peltonen (1990) related the negative Ni_{OL}-Fo trend to the volume of metamorphic olivine produced by dehydration reactions. The presence of sulfides during recrystallization may have some effect to the Ni_{OL}-Fo relationship in the Group 2 inclusions.

Overall, the olivine compositions are somewhat lower in Fo (generally $Fo_{79.9\text{-}84.4}$) than expected for komatiitic rocks ($Fo_{>90}$) and also lower than expected for metamorphic olivine formed through deserpentinization reactions. Breakdown of chlorite has been invoked to explain the Fe-rich nature of olivine porphyroblasts found in metamorphosed

ultramafic metavolcanic rocks (Oliver et al., 1972; Peltonen, 1990). Chloritic schists occur as country rocks to the Kevitsa intrusion as part of the ultramafic metavolcanic rocks and thus its decomposition may have been responsible for the composition of the porphyroblastic olivine in Group 2 inclusions.

7.6. Role of the inclusions in the sulfide ore genesis

Yang et al. (2013) explained the Ni-enriched olivine in the Kevitsa Ni-PGE ore type by assimilation of Ni-rich sulfides from dunitic xenoliths and related the formation of the dunite inclusions to an early-stage komatiitic magmatism. This model is in line with the present study suggesting a close temporal link between the emplacement of the Central Dunite and Kevitsa olivine-pyroxenites. The model, however, comes with some problems. The authors regarded the Ni-rich sulfides found as "interstitial" as a primary feature, leading to the interpretation of interaction of the komatiitic sulfide phase with Kevitsa magma. As discussed here, particularly the Group 1 sulfide-bearing inclusions tend to be found within sulfide-bearing host rocks and with similar sulfide assemblage. Based on this observation, we argue that sulfides infiltrated into the inclusions and are thus not necessarily a primary feature of the inclusions. Assuming that the Central Dunite is an expression of the komatiitic magma conduit, we would expect to find evidence for a sulfide saturation event from the dunitic cumulates, but this is not the case. The model by Yang et al. (2013) does not take into account the peculiar LREE-enriched nature of the host rocks of the Ni-PGE ore type, which, based on this study, could not result from assimilation of any inclusion type discussed here. Le Vaillant et al. (2015) also noted elevated Pd/Ir and Pt/Ir in Ni-PGE ore, which are inconsistent with assimilation of komatiitic Ni sulfides, as these would rather decrease the Pt/Ir and Pd/Ir ratios.

The Kevitsa Dunite occurs in the core of the deposit and overall, the recrystallized inclusions are far more abundant within the ore-bearing part of the Kevitsa intrusion than elsewhere. The role of the inclusions or the Kevitsa Dunite in the genesis of the sulfide ore is enigmatic. The occurrence of the inclusions and xenoliths within the sulfide-ore bearing part of the intrusion indicate a site of vigorous and dynamic emplacement of magma. The concentration of a high number of inclusions and entrapment of the Kevitsa Dunite must have increased the viscosity and thus decreased the flow rate of the Kevitsa magma. This may have evoked settling of the sulfides. Aside from the sulfidic shales, the mafic-ultramafic volcanic rocks of the Group 2 inclusion type may have provided additional sulfur to the Kevitsa magma.

8. Geological model

On the basis of this study, a multi-phase emplacement history of the Kevitsa intrusive suite is proposed and the origin of the dunitic cumulates and ultramafic recrystallized inclusions are summarized as follows:

1) Hydrous picritic magma intruded as vertical dikes and horizontal sills forming the Central Dunite body (Fig. 14a). The magma was saturated in olivine and chromite and formed dunite adcumulates probably by flow differentiation. Poikilitic wehrlites and feldspathic wehrlites formed either from expelled intercumulus liquid during compaction of the olivine-chromite adcumulate (annealing) or as a response of evolving magma composition. Most of the magma escaped and is currently found as picritic lavas in central Finnish Lapland.

2) Magma in the lower staging chamber underwent fractionation and/or became more crustally contaminated due to assimilation of country rocks. The evolved basaltic magma (Kevitsa magma) intruded the same route and crystallized olivine-pyroxene cumulates (Fig. 14b).

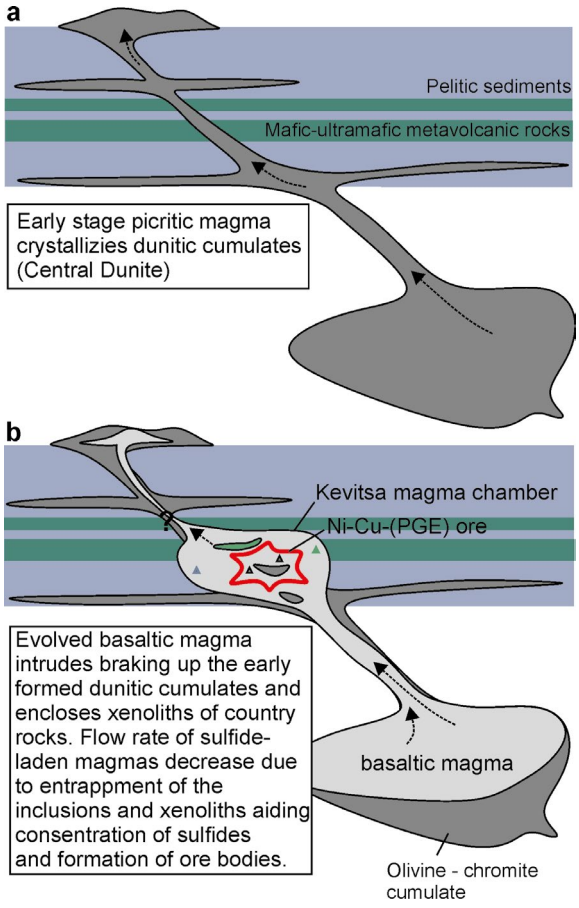

Figure 14. Integrated geological model for the formation of Kevitsa intrusive suite rocks.

3) A large "slice" of the early-formed dunitic cumulates became trapped and brecciated within the Kevitsa magma chamber (Kevitsa Dunite). Due to the added heat, hydrous minerals and plagioclase melted and the rocks reacted with their surroundings. Small brecciated clasts recrystallized to polygonal olivine-clinopyroxene-chromite aggregates forming Group 1 inclusions.

4) Xenoliths of mafic-ultramafic metavolcanic country rocks underwent thermal metamorphism and formed Group 2 inclusions.

5) The entrapment of the Kevitsa Dunite and numerous inclusions decreased the flow rate of the sulfide-bearing Kevitsa magmas and evoked concentration of the sulfides, contributing to the formation of the Ni-Cu-PGE ore.

9. Conclusions

The main points of our field (drill-core), petrological and geochemical investigations of the dunitic rocks in the Kevitsa intrusion are:

– The Central Dunite comprises olivine-chromite cumulates and represents a separate magmatic body in a close association with the Kevitsa intrusive succession.

– The obtained olivine compositions of $Fo_{85.1\text{-}88.6}$ and similar LREE-enriched REE characteristics to the picritic volcanic rocks in the Savukoski Group suggest a picritic parental magma for the Central Dunite.

– Large inclusions of dunitic cumulates are also found hosted by the Ni-Cu sulfide ore-bearing part of the Kevitsa intrusion. These inclusions are mineralogically and compositionally comparable to the Central Dunite and interpreted as rafts of Central Dunite trapped within later-invading Kevitsa magma.

– The similar mildly LREE-enriched REE characteristics and systematic relationship between whole-rock and mineral compositions between the Central Dunite and Kevitsa olivine pyroxenites indicate that these rocks are genetically related.

– Apart from the cumulate-textured dunitic rocks, numerous recrystallized olivine-dominated inclusions are found within the Kevitsa

intrusion, showing chemical affinity either towards the dunitic cumulates (Group 1) or the mafic-ultramafic volcanogenic country rocks in the area (Group 2).

– The Group 1 inclusions comprise olivine-chromite-clinopyroxene aggregates with highly heterogeneous mineral compositions with no correlations between Ni and Fo in olivine or Cr and Mg# in clinopyroxene. Their REE characteristics mimick those observed in their host olivine pyroxenites. These features may be explained by the presence of relict, neoblastic and metamorphic olivine and by local equilibration with the host rocks.

– The Group 2 inclusions consist in variable modes of olivine, clinopyroxene, orthopyroxene, and oxides with or without plagioclase, amphibole, and sulfides. Their hump-shaped REE patters are similar to those of the Savukoski Group komatiitic volcanic rocks. The olivine compositions ($<Fo_{85}$) in Group 2 inclusions are somewhat lower than expected for komatiitic rocks or for metamorphic olivine formed by deserpentinization reactions. Porphyroblastic olivine in Group 2 inclusions is interpreted to originate from dehydration of chlorite (decomposition of chloritic metavolcanic country rocks).The ultramafic inclusions are most abundant within the ore-bearing domain of the Kevitsa intrusion.

– The role of the inclusions to the ore formation is ambiguous but it is proposed here that the entrapment of a high number of inclusions decreased the flow rate of the sulfide-bearing Kevitsa magma, aiding the gravitational settling of sulfide droplets.

Acknowledgements

During the course of this study, the ownership of the Kevitsa mine changed from First Quantum Minerals Limited (FQM Ltd) to Boliden AB. We are grateful to both companies for providing access to the drill cores and database. Financial support for this study was obtained from First Quantum Minerals Ltd (FQM), the Academy of Finland (#281859), and K.H. Renlund Foundation. Markku Lappalainen (FQM Ltd) and Petri Peltonen, Teemu Voipio and Teemu Lehtilä (former FQM Ltd) are thanked for discussions and support of the research. The authors would also like to thank Sofia Chistyakova, Tapio Halkoaho and Geoffrey Howarth for their thoughtful and constructive reviews. Leena Palmu is thanked for help with microprobe analyses.

Supplementary data

Electronic Appendices A–C for this article are available via Bulletin of the Geological Society of Finland web page.

References

Arai, S., 1975. Contact metamorphosed dunite-harzburgite complex in the Chugoku district, western Japan. Contributions to Mineralogy and Petrology 52, 1–16. https://doi.org/10.1007/BF00377998

Ashley, P.M., Ambler, E.P. & Flood, R.H., 1979. Two occurrences of ultramafic hornfels in the Biggenden Beds, southeastern Queensland. Journal of the Geological Society of Australia 26, 29–37. https://doi.org/10.1080/00167617908729064

Barnes, S.J., 1986. The effect of trapped liquid crystallization on cumulus mineral compositions in layered intrusions. Contributions to Mineralogy and Petrology 93, 524–531. https://doi.org/10.1007/BF00371722

Barnes, S.J., Hill, R.E.T. & Gole, M.J., 1988. The Perseverance Ultramafic Complex, Western Australia: The product of a komatiite lava river. Journal of Petrology 29, 305–331. https://doi.org/10.1093/petrology/29.2.305

Barnes, S.-J. & Lightfoot, P., 2005. Formation of magmatic nickel-sulfide ore deposits and processes affecting their copper and platinum-group element contents. In: Hedenquist, J.W., Thompson, J.F.H., Goldfarb, R.J. & Richards, J.P. (eds.), Society of Economic Geologist, INC. Economic Geology 100th Anniversary Volume 1905–2005, pp. 179–213.

Bèdard, J.H., Sparks, R.S.J., Renner, R., Cheadle, M.J. & Hallworth, M.A., 1988. Peridotite sills and metasomatic gabbros in the Eastern Layered Series of the Rhum Complex. Journal of the Geological Society of London 145, 207–224. https://doi.org/10.1144/gsjgs.145.2.0207

Bliss, N.W. & MacLean, W.H., 1975. The paragenesis of zoned chromite from central Manitoba. Geochimica et Cosmochimica Acta 39, 973–990. https://doi.org/10.1016/0016-7037(75)90042-3

Bushey, J.C., Snoke, A.W., Barnes, C.G. & Frost, C.D., 2006. Geology of the Bear Mountain intrusive complex, Klamath Mountains, California. Special Paper of the Geological Society of America 410, 287–315. https://doi.org/10.1130/2006.2410(14)

Chai, G. & Naldrett, A.J., 1992. The Jinchuan ultramafic intrusion: Cumulate of a high-Mg basaltic magma. Journal of Petrology 33, 277–303. https://doi.org/10.1093/petrology/33.2.277

Grinenko, L.N., Hanski, E. & Grinenko, V.A., 2003. Formation conditions of the Keivitsa Cu-Ni deposit, northern Finland: Evidence from S and C isotopes. Geochemistry International 41, 154–167.

Hanski, E. & Huhma, H., 2005. Central Lapland greenstone belt. In: Lehtinen, M., Nurmi, P.A. & Rämö, O.T. (ed.), Precambrian Geology of Finland – Key to the Evolution of the Fennoscandian Shield. Developments in Precambrian Geology 14, Elsevier, Amsterdam, pp. 139–193. https://doi.org/10.1016/S0166-2635(05)80005-2

Hanski, E. & Kamenetsky, V.S., 2013. Chrome spinel-hosted melt inclusions in Paleoproterozoic primitive volcanic rocks, northern Finland: Evidence for coexistence and mixing of komatiitic and picritic magmas. Chemical Geology 343, 25–37. https://doi.org/10.1016/j.chemgeo.2013.02.009

Hanski, E.J., Huhma, H., Suominen, I.M. & Walker, R.J., 1997. Geochemical and isotopic (Os, Nd) study of the early Proterozoic Keivitsa Intrusion and its Cu-Ni deposit, northern Finland. In: Papunen, H. (ed.), Mineral Deposits: Research and Exploration—Where Do They Meet? Proceedings of 4th Biennial SGA Meeting, Finland. A.A. Balkema, Rotterdam, pp. 435–438.

Hanski, E., Huhma, H., Rastas, P. & Kamenetsky, V.S., 2001. The Palaeoproterozoic komatiite-picrite association of Finnish Lapland. Journal of Petrology 42, 855–876. https://doi.org/10.1093/petrology/42.5.855

Feig, S.T., Koepke, J. & Snow, J.E., 2006. Effect of water on tholeiitic basalt phase equilibria: An experimental study under oxidizing conditions. Contributions to Mineralogy and Petrology 152, 611–638. https://doi.org/10.1007/s00410-006-0123-2

Howarth, G.H. & Prevec, S.A., 2013. Hydration vs. oxidation: Modelling implications for Fe–Ti oxide crystallisation in mafic intrusions, with specific reference to the Panzhihua intrusion, SW China. Geoscience Frontiers 4, 555–569. https://doi.org/10.1016/j.gsf.2013.03.002

Irvine, T.N., 1974. Petrology of the Duke Island ultramafic complex, southeastern Alaska. Memoir of the Geological Society of America 138. https://doi.org/10.1130/MEM138-p1

Irvine, T., 1980. Magmatic infiltration metasomatism, double-diffusive fractional crystallization, and adcumulus growth in the Muskox Intrusion and other layered intrusions. In: Hargraves, R.B (ed.), Physics of Magmatic Processes, Princeton University Press, New Jersey, United States, pp. 325–384.

Khedr, M.Z. & Arai, S., 2012. Petrology and geochemistry of prograde deserpentinized peridotites from Happo-O'ne, Japan: Evidence of element mobility during deserpentinization. Journal of Asian Earth Sciences 43, 150–163. https://doi.org/10.1016/j.jseaes.2011.08.017

Klügel, A., 1998. Reactions between mantle xenoliths and host magma beneath La Palma (Canary Islands); constraints on magma ascent rates and crustal reservoirs. Contributions to Mineralogy and Petrology 131, 237–257. https://doi.org/10.1007/s004100050391

Koivisto, E., Malehmir, A., Hellqvist, N., Voipio, T. & Wijns, C., 2015. Building a 3D model of lithological contacts and near-mine structures in the Kevitsa mining and exploration site, Northern Finland: Constraints from 2D and 3D reflection seismic data. Geophysical Prospecting

63, 754–773.
https://doi.org/10.1111/1365-2478.12252

Kunugiza, K., 1980. Dunites and serpentinites in the Sanbagawa metamorphic belt, central Shikoku and Kii Peninsula, Japan. Journal of the Japanese Association of Mineralogists, Petrologists & Economic Geologists 75, 14–24.
https://doi.org/10.2465/ganko1941.75.14

Le Vaillant, M., Barnes, S.J., Fiorentini, M.L., Santaguida, F. & Törmänen, T., 2016. Effects of hydrous alteration on the distribution of base metals and platinum group elements within the Kevitsa magmatic nickel sulphide deposit. Ore Geology Reviews 72, 128–148.
https://doi.org/10.1016/j.oregeorev.2015.06.002

Lehtonen, M., Airo, M.-L., Eilu, P., Hanski, E., Kortelainen, V., Lanne, E., Manninen, T., Rastas, P., Räsänen, J. & Virransalo, P., 1998. The stratigraphy, petrology and geochemistry of the Kittilä greenstone area, northern Finland: A report of the Lapland Volcanite Project. Geological Survey of Finland, Report of Investigation 140 (in Finnish with English summary)

Li, C. & Naldrett, A.J., 1999. Geology and petrology of the Voisey's Bay intrusion: reaction of olivine with sulfide and silicate liquids. Lithos 47, 1–31.
https://doi.org/10.1016/S0024-4937(99)00005-5

McCallum, I.S., 1996. The Stillwater Complex. Developments in Petrology 15, 441–483.
https://doi.org/10.1016/S0167-2894(96)80015-7

Mercier, J.-C. & Nicolas, A., 1975. Textures and fabrics of upper-mantle peridotites as illustrated by xenoliths from basalts. Journal of Petrology 16, 454–487.
https://doi.org/10.1093/petrology/16.1.454

Mutanen, T., 1997. Geology and ore petrology of the Akanvaara and Koitelainen mafic layered intrusions and the Keivitsa-Satovaara layered complex, northern Finland. Geological Survey of Finland, Bulletin 395, 233 p.

Mutanen, T. & Huhma, H., 2001. U-Pb geochronology of the Koitelainen, Akanvaara and Keivitsa layered intrusions and related rocks. Special Paper - Geological Survey of Finland 33, 229–246.

Nozaka, T., 2003. Compositional heterogeneity of olivine in thermally metamorphosed serpentinite from Southwest Japan. American Mineralogist 88, 1377–1384.
https://doi.org/10.2138/am-2003-8-922

Nozaka, T., 2010. A note on compositional variation of olivine and pyroxene in thermally metamorphosed ultramafic complexes from SW Japan. Okayama University Earth Science Reports 17, 1–5.

Nozaka, T. & Shibata, T., 1995. Mineral paragenesis in thermally metamorphosed serpentinites, Ohsa-yama, Okayama Prefecture. Okayama University Earth Science Reports 2, 1–12.

Oliver, R.L., Nesbitt, R.W., Hausen, D.M. & Franzen, N., 1972. Metamorphic olivine in ultramafic rocks from Western Australia. Contributions to Mineralogy and Petrology 36, 335–342.
https://doi.org/10.1007/BF00444340

Paktunc, A.D., 1984. Metamorphism of the ultramafic rocks of the Thompson Mine, Thompson nickel belt, northern Manitoba**.** Canadian Mineralogist 22, 77–91.

Peltonen, P., 1990. Metamorphic olivine in pictritic metavolcanics from southern Finland. Bulletin of the Geological Society of Finland 62, 99–114.
https://doi.org/10.17741/bgsf/62.2.001

Raedeke, L.D. & Mccallum, I.S., 1984. Investigations in the Stillwater Complex: Part II. Petrology and petrogenesis of the ultramafic series. Journal of Petrology 25, 395–420.
https://doi.org/10.1093/petrology/25.2.395

Rasilainen, K., Lahtinen, R. & Bornhorst, T.J. 2007. The Rock Geochemical Database of Finland Manual. Geological Survey of Finland, Report of Investigation 164, 38 p.

Rehfeldt, T., Jacob, D.E., Carlson, R.W. & Foley, S.F., 2007. Fe-rich dunite xenoliths from South African kimberlites: Cumulates from Karoo flood basalts. Journal of Petrology 48, 1387–1409.
https://doi.org/10.1093/petrology/egm023

Roeder, P.L. & Emslie, R.F., 1970. Olivine–liquid equilibrium. Contributions to Mineralogy and Petrology 29, 275–289.
https://doi.org/10.1007/bf00371276

Santaguida, F., Luolavirta, K., Lappalainen, M., Ylinen, J., Voipio, T. & Jones, S., 2015. The Kevitsa Ni-Cu-PGE Deposit in the Central Lapland Greenstone Belt in Finland. In: Maier, W., O'Brien, H. & Lahtinen, R. (eds.), Mineral Deposits of Finland. Elsevier, Amsterdam, pp. 195–210.
https://doi.org/10.1016/B978-0-12-410438-9.00008-X

Säntti, J., Kontinen, A., Sorjonen-Ward, P., Johanson, B. & Pakkanen, L., 2006. Metamorphism and chromite in serpentinized and carbonate-silica-altered peridotites of the Paleoproterozoic Outokumpu-Jormua ophiolite belt, eastern Finland. International Geology Review 48, 494–546.
https://doi.org/10.2747/0020-6814.48.6.494

Schiffries, C.M., 1982. The petrogenesis of a platiniferous dunite pipe in the Bushveld Complex: infiltration metasomatism by a chloride solution. Economic Geology 77, 1439–1453.
https://doi.org/10.2113/gsecongeo.77.6.1439

Scoon, R.N. & Mitchell, A.A., 2004. Petrogenesis of discordant magnesian dunite pipes from the central sector of the eastern Bushveld Complex with emphasis on the Winnaarshoek Pipe and disruption of the Merensky Reef. Economic Geology 99, 517–541. https://doi.org/10.2113/gsecongeo.99.3.517

Scoon, R.N. & Mitchell, A.A., 2009. A multi-stage orthomagmatic and partial melting hypothesis for the Driekop platiniferous dunite pipe, eastern limb of the Bushveld Complex, South Africa. South African Journal of Geology 112, 163–186. https://doi.org/10.2113/gssajg.112.2.163

Sobolev, A.V., Hofmann, A.W., Sobolev, S.V. & Nikogosian, I.K., 2005. An olivine-free mantle source of Hawaiian shield basalts. Nature 434, 590–597.
https://doi.org/10.1038/nature03411

Sørensen, H.S. & Wilson, J.R., 1996. Petrology of the Treknattan Intrusion in the Fongen-Hyllingen Complex, Trondheim region, Norway; a late intrusion into an evolved layered complex. Lithos 38, 109–127. https://doi.org/10.1016/0024-4937(96)00013-8

Springer, R.K., 1974. Contact metamorphosed ultramafic rocks in the western Sierra Nevada foothills, California. Journal of Petrology 15, 160–195. https://doi.org/10.1093/petrology/15.1.160

Straub, S.M., LaGatta, A.B., Martin-Del Pozzo, A.L. & Langmuir, C.H., 2008. Evidence from high-Ni olivines for a hybridized peridotite/pyroxenite source for orogenic andesites from the central Mexican Volcanic Belt. Geochemistry, Geophysics, Geosystems 9, Q03007. https://doi.org/10.1029/2007GC001583

Straub, S.M., Gomez–Tuena, A., Stuart, F.M., Zellmer, G.F., Espinasa–Perena, R., Cai, Y. & Iizuka, Y., 2011. Formation of hybrid arc andesites beneath thick continental crust. Earth and Planetary Science Letters 303, 337–347. https://doi.org/10.1016/j.epsl.2011.01.013

Stumpfl, E.F. & Rucklidge, J.C., 1982. The platiniferous dunite pipes of the eastern Bushveld. Economic Geology 77, 1419–1431. https://doi.org/10.2113/gsecongeo.77.6.1419

Sun, S.-S. & McDonough, W.F., 1989. Chemical and isotopic systematics of oceanic basalts: implications for mantle composition and processes. Geological Society of London Special Publication 42, 313–345. https://doi.org/10.1144/GSL.SP.1989.042.01.19

Tegner, C. & Robins, B., 1996. Picrite sills and crystal-melt reactions in the Honningsvåg intrusive suite, Northern Norway. Mineralogical Magazine 60, 53–66. https://doi.org/10.1180/minmag.1996.060.398.05

Tegner, C. & Wilson, J.R., 1993. A late ultramafic suite in the Kap Edvard Holm layered gabbro complex, East Greenland. Geological Magazine 130, 431–442. https://doi.org/10.1017/S0016756800020513

Tuff, J., Takahashi, E. & Gibson, S.A., 2005. Experimental constraints on the role of garnet pyroxenite in the Genesis of high-Fe mantle plume derived melts. Journal of Petrology 46, 2023–2058. https://doi.org/10.1093/petrology/egi046

Vance, J.A. & Dungan, M.A., 1977. Formation of peridotites by deserpentinization in the Darrington and Sultan areas, Cascade Mountains, Washington. Bulletin of the Geological Society of America 88, 1497–1508. https://doi.org/10.1130/0016-7606(1977)88

Wang, C.Y., Zhou, M. & Zhao, D., 2005. Mineral chemistry of chromite from the Permian Jinbaoshan Pt-Pd-sulphide-bearing ultramafic intrusion in SW China with petrogenetic implications. Lithos 83, 47–66. https://doi.org/10.1016/j.lithos.2005.01.003

Yang, S., Maier, W.D., Hanski, E.J., Lappalainen, M., Santaguida, F. & Määttä, S., 2013. Origin of ultra-nickeliferous olivine in the Kevitsa Ni-Cu-PGE-mineralized intrusion, northern Finland. Contributions to Mineralogy and Petrology 166, 81–95. https://doi.org/10.1007/s00410-013-0866-5